

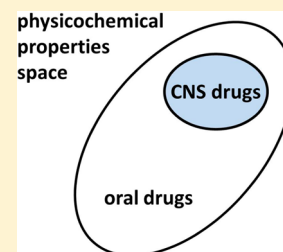
CNS Drug Design: Balancing Physicochemical Properties for Optimal Brain Exposure

Zoran Rankovic*

Eli Lilly and Company, 893 South Delaware Street, Indianapolis, Indiana 46285, United States

S Supporting Information

ABSTRACT: The human brain is a uniquely complex organ, which has evolved a sophisticated protection system to prevent injury from external insults and toxins. Designing molecules that can overcome this protection system and achieve optimal concentration at the desired therapeutic target in the brain is a specific and major challenge for medicinal chemists working in CNS drug discovery. Analogous to the now widely accepted rule of 5 in the design of oral drugs, the physicochemical properties required for optimal brain exposure have been extensively studied in an attempt to similarly define the attributes of successful CNS drugs and drug candidates. This body of work is systematically reviewed here, with a particular emphasis on the interplay between the most critical physicochemical and pharmacokinetic parameters of CNS drugs as well as their impact on medicinal chemistry strategies toward molecules with optimal brain exposure. A summary of modern CNS pharmacokinetic concepts and methods is also provided.



1. INTRODUCTION

Traditionally, the development of medicines for central nervous system (CNS) disorders has been an intense and profitable research activity for the pharmaceutical industry. Despite the recent divestment of research in some areas, such as psychiatric disorders (i.e., depression and schizophrenia),¹ this trend is likely to continue as a result of the acute medical needs and market opportunities created by an increasing human life span. It is estimated that, in the absence of disease-modifying treatments, age-related neurodegenerative conditions such as Alzheimer's disease and Parkinson's disease will be the major drivers of the predicted increase in US health care expenditures from the current ~15% of gross domestic product (GDP) to ~29% of GDP in 2040.² Additionally, the brain is a common site of metastases for some of the most prevalent cancers, such as lung and breast cancers,³ and is the second leading cause of death in the United States among males younger than 40 years and females younger than 20 years.⁴ Patients who present with metastatic brain cancer have a poor prognosis with a median survival of only 2.5 months,⁵ which is at least partially a consequence of poor CNS exposure for currently available drugs that were developed to treat systemic disease. Consequently, CNS exposure is increasingly seen as an important requirement in the development of new cancer treatments.⁶

However, the pressures of medical needs and the incentives of market opportunities are countered by the challenges and complexities of CNS drug discovery. In addition to the difficulties of CNS target validation and clinical translation, designing therapeutic agents that are able to reach and effectively modulate targets in the brain makes CNS research one of the most challenging endeavors in drug discovery. This is largely due to a highly sophisticated protection system that the brain has evolved to preserve its physiological environment and shield itself from external insults and toxins. An important component

of this system is the blood–brain barrier (BBB), which lies at the interface between the blood capillaries of the brain and brain tissue.⁷ The BBB has a very complex multicellular organization comprising brain endothelial cells that line the blood vessels and form the brain capillary endothelium as well as surrounding cells, including pericytes, astrocytes, and neurons. The BBB provides a fully autonomous milieu for the cells within the CNS, enabling selective access of required nutrients and hormones while removing waste and diminishing exposure to potentially harmful xenobiotics.⁷ The blood–cerebrospinal fluid barrier (BCSFB) is a similar barrier between the blood capillaries and the cerebrospinal fluid (CSF), which fills the ventricles and bathes the external surface of the brain to provide buoyancy and mechanical protection within the skull.⁸ In brain tissue, the CSF is exchanged with the brain's interstitial fluid (ISF), which eliminates metabolic waste from the CNS and regulates the chemical environment of the brain (Figure 1).

Since the density of the capillaries within the brain parenchyma is so high that virtually every neuron is supplied by its own capillary (the combined capillary length in the human brain is 400 miles), it is estimated that the BBB surface area (~120 square feet) is approximately 5000 times larger than the BCSFB surface area. Consequently, the BBB is thought to have a much greater role than the BCSFB in CNS drug delivery to the brain.^{9,10} Active transport and passive diffusion through endothelial cells are the two principal mechanisms by which molecules can enter the brain. In contrast to the endothelial cells of capillaries elsewhere in the body, diffusion through the intercellular space between cells (paracellular) is effectively precluded by the presence of the tight junctions that characterize the BBB and BCSFB. For example, the capillary

Received: October 5, 2014

Published: December 11, 2014

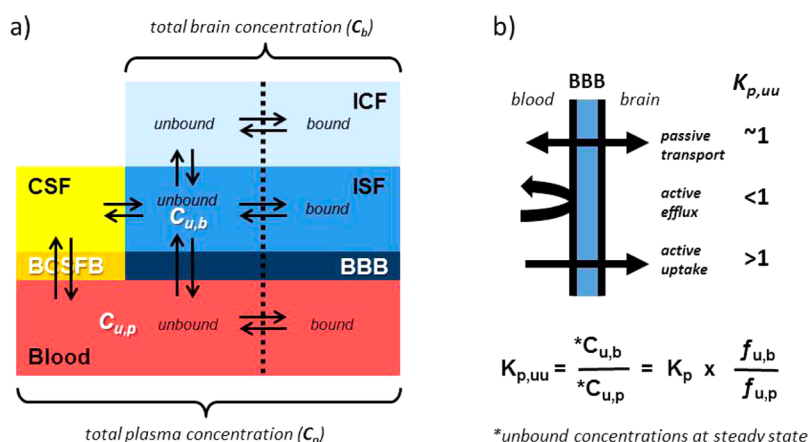


Figure 1. Principal CNS PK parameters and concepts. (a) Schematic representation of bound and unbound drug concentration equilibrium across BBB and brain main compartments: interstitial fluid (ISF), intracellular fluid (ICF), and cerebrospinal fluid (CSF); (b) $K_{p,uu}$ values significantly lower or higher than 1 indicate active transport across the BBB.

endothelial cell junctions in the brain are sufficiently tight to restrict the movement of ions such as Na^+ and Cl^- and consequently display much higher transendothelial electrical resistance than peripheral capillaries (>1000 versus <20 ohm/ cm^2).¹¹ This restrictiveness is thought to protect the brain from fluctuations in ionic composition that may occur, e.g., during a meal or physical activity.

The majority of CNS drugs are small molecules that cross the BBB via the transcellular passive diffusion route.¹² Designing molecules that can achieve optimal concentration at the desired therapeutic target in the brain is a unique and major challenge for medicinal chemists working in CNS drug discovery.^{13–15} Tremendous progress has been made in recent years in terms of enabling the development of robust pharmacokinetic-pharmacodynamic (PK/PD) relationships for centrally acting agents as well as in understanding how these relationships are influenced by molecular physicochemical properties. The objective of this Perspective is to review this progress and highlight successful medicinal chemistry strategies toward molecules that can achieve optimal brain exposure via transcellular passive diffusion. Alternative brain delivery systems utilizing BBB active transport are beyond the scope of this Perspective, and the reader is referred to an excellent review of this topic.¹⁶

At this point, it should also be noted that the term “optimal” is used loosely in this context, since there is no single value or desirable concentration range, but what is considered to be optimal exposure depends on a multitude of variables, including drug potency, mode of action (e.g., agonist vs antagonist), binding kinetics (e.g., fast vs slow dissociation constant or reversible vs irreversible binders), pharmacokinetic properties, and therapeutic index. One could define the optimal brain exposure as a free drug concentration at the site of the intended target expressed in the brain that produces maximum desired and minimum undesired effects (best therapeutic window) over the time course deemed to be suitable for the intended dosing regimen (e.g., once-a-day).

2. IMPORTANT CNS PHARMACOKINETIC CONCEPTS AND PARAMETERS

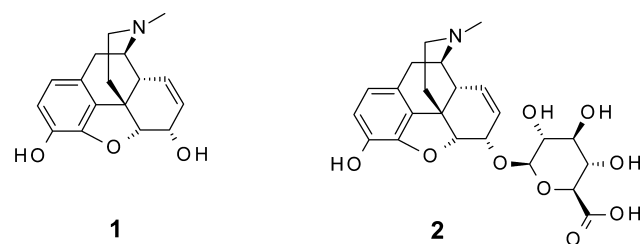
Achieving a good understanding of the PK and PD relationships in preclinical disease models, which is a critical prerequisite for successful drug discovery programs across all therapeutic areas,

is particularly challenging for CNS targets. The existence of the BBB renders classical PK parameters, such as oral bioavailability and plasma concentration, insufficient for assessing drug exposure and time courses in the brain. For a meaningful assessment of CNS drug candidates, additional data and more sophisticated PK methods are required.^{17–21}

2.1. Free Drug Hypothesis. The most direct information on drug exposure at the site of action is provided by receptor occupancy (RO) studies. In the clinical setting, brain RO is measured using radiolabeled tracer ligands whose distribution can be determined by noninvasive imaging methods, such as single photon emission computed tomography (SPECT) and positron emission tomography (PET).²² In preclinical studies, the tracer distribution is established mainly by scintillation spectroscopy of dissected brain tissue. These studies are characterized by the need for radiolabeled ligands, long turnaround times, and relatively low success rates (particularly for agonists). Therefore, due to technical complexities as well as time and costs involved, RO studies tend to be performed mainly for the most advanced compounds. Consequently, the more easily obtained drug total brain concentration (C_b) and whole brain-to-plasma ratio ($K_p = C_b/C_p$; also referred to as the B/P ratio) have historically been used as the main decision-making drivers in CNS drug discovery.

However, recent evidence suggests that relying solely on these parameters is insufficient for adequate understanding of the CNS exposure needed to establish robust PK/PD correlations.²³ This insufficiency arises from the fact that only a fraction of total drug concentration in the plasma (C_p) and tissues, such as brain (C_b), is unbound from the tissue proteins or lipids and is free to diffuse across biological barriers and tissues to reach the intended therapeutic target ($C_{u,p} = C_p \times f_{u,p}$ and $C_{u,b} = C_b \times f_{u,b}$, respectively), as depicted in Figure 1a. Because the unbound plasma and tissue fractions tend to be different, the unbound brain-to-plasma ratio ($K_{p,uu}$) is often considerably different from the total brain-to-plasma ratio (K_p).

The potential for misleading conclusions derived from the reliance on total brain and plasma concentrations is well-exemplified by comparative *in vivo* PK/PD studies of morphine, **1**, and one of its active metabolites, morphine-6-glucuronide **2** (M6G).²⁴ Both compounds are thought to exert their centrally mediated analgesic affect through the activation of mu-opioid receptors (MOR) expressed in CNS.

Table 1. Morphine and Morphine-6-glucuronide Paradox Explained by Considering Drug $C_{u,b}$ Data^{27,28}

compd	MOR ^a K_i (nM)	AUC _b ^b (μ M/min)	K_p	ISF AUC ^c (μ M/min)	$K_{p,uu}$
1	22	186	0.74	79	0.51
2	63	42	0.05	336	0.56

^a[³H]-Naloxone displacement binding assay in MOR-expressing cell membranes.²⁵ ^bTotal brain AUC concentration in rat, 10 mg/kg (s.c.). ^cMeasured by *in vivo* transcortical microdialysis.²⁸

Although the two compounds exhibit similar activities *in vitro* (Table 1),²⁵ their similar *in vivo* efficacy²⁶ was unexpected considering the poor total brain/plasma ratio ($K_p = 0.05$) and much lower rate of BBB permeation, expressed as permeability surface area product (PS = 0.11 μ L/min/g), for **2** compared with those of morphine ($K_p = 0.54$; PS = 3.5 μ L/min/g). In fact, based on the classic concepts of CNS exposure, **2** should have no *in vivo* efficacy.²⁷ To explain this phenomenon, several hypotheses, such as glucuronide **2** activation of a new and not yet discovered receptor subtype, have been proposed.²⁴ However, this apparent paradox could also be explained by considering the unbound (free) rather than total drug concentrations in the brain.²⁸ Actually, whereas the **2** total brain AUC concentration is 4–5-fold lower compared with that of morphine, the drug ISF AUC (unbound) is approximately 4-fold higher than morphine (Table 1), which may explain the similar *in vivo* efficacy observed for these two compounds.²⁷ These general observations have been confirmed by multiple CNS drug studies reported over the past decade: ISF is the relevant brain compartment for drug pharmacodynamics effect, and ISF drug concentration is not reflected by the total brain concentration.^{15,23,27}

It is important to note that the total B/P ratio (K_p) can be misleading, even when comparing structurally similar compounds. For example, a K_p value of 0.04 suggests significantly lower brain penetration for (*R*)-cetirizine compared with that of its enantiomer, (*S*)-cetirizine, which has a K_p value of 0.22.²⁹ However, the unbound drugs in the brain ($C_{u,b}$) and plasma ($C_{u,p}$) show that (*S*)- and (*R*)-cetirizine have very similar, if not identical, effective compound levels in the brain, with $K_{p,uu}$ ($C_{u,b}/C_{u,p}$) values of 0.17 and 0.14, respectively. The observed K_p enantioselectivity has been rationalized by the lower plasma protein binding (PPB) of (*S*)-cetirizine (PPB = 50%) compared with that of (*R*)-cetirizine (PPB = 85%).²⁹

The importance of free drug concentrations is embedded in the central tenet of *in vivo* pharmacology, the free drug hypothesis, which states that: (1) the free (unbound) drug concentration (C_u) at the site of action is responsible for pharmacological activity *in vivo* and (2) at steady state and in the absence of active transport, the free drug concentration is the same on both sides of any biomembrane (e.g., the BBB).³⁰ Thus, at steady state, one could equate the drug unbound brain concentration ($C_{u,b}$) with its experimentally more accessible unbound plasma concentration ($C_{u,p}$). The $C_{u,p}$ could be then

used in combination with the drug *in vitro* potency data to estimate the brain exposure or dose required for *in vivo* efficacy. However, it is important to note that this assumption is not valid for compounds that

- Display a low rate of passive permeability across the BBB/BCSFB (require a long time to reach equilibrium across membranes).
- Are actively transported in or out of the brain.

In these cases, the disconnect between a compound's free plasma and brain concentrations ($C_{u,b} \neq C_{u,p}$) is translated into $K_{p,uu}$ values, which can be either above or below 1. $K_{p,uu}$ values below 1 indicate compounds that are subject to active efflux and/or have low passive permeability across the BBB (Figure 1b).³¹ This profile is suitable for peripherally active drugs, such as (*S*)-cetirizine ($K_{p,uu} = 0.22$), a second-generation antihistamine that was intentionally designed to minimize brain exposure to avoid sedation and other CNS side effects generally associated with first-generation antihistamines.³² However, pursuing compounds with low $K_{p,uu}$ values for CNS targets is less desirable, due not only to the higher peripheral exposure needed to achieve efficacious brain levels and the consequently increased risk of side effects but also to the difficulty with estimating low human $C_{u,b}$, which results in low confidence human dose predictions.²³ $K_{p,uu}$ values greater than 1, as exemplified by the first-generation antihistamine diphenhydramine (rat $K_{p,uu} = 5.5$), indicate an active uptake process mediated by influx transporters.³³ Active transport may offer an alternative approach for achieving optimal brain exposure for molecules whose properties are nonconductive to passive BBB penetration, as exemplified by gabapentin or L-DOPA that are transported via L-type amino acid transporter-1 (LAT1).³⁴ However, intentionally targeting specific transport proteins or transcytosis mechanisms for CNS drug delivery remains challenging, and, although this approach has attracted interest across the pharmaceutical industry and academia, research in this area is still in its infancy.¹⁶ A successful small molecule CNS drug candidate typically complies with the free drug hypothesis and displays a ratio of the unbound drug in the brain to the unbound drug in the plasma ($K_{p,uu}$ value) close to 1.^{19,35} With a $K_{p,uu}$ in mouse of 0.98, the antidepressant venlafaxine is one such example.³⁶

To simplify the process and increase the throughput, $K_{p,uu}$ values are often estimated from single-time-point measurements. This is generally an acceptable approximation; however, one should be aware that such data can be misleading if the selected time point was before the system could reach steady state. In this context, more reliable $K_{p,uu}$ values are generated using the area under the concentration–time curves (AUCs) for total and unbound concentrations obtained from time course experiments ($K_{p,uu} = \text{AUC}_{u,b}/\text{AUC}_{u,p}$). Again, AUCs and steady-state concentrations can be used interchangeably in this equation as they measure the same property.³⁶ When making important decisions on the basis of $K_{p,uu}$ data, it is worth remembering that these values include experimental errors from four separate *in vivo* and *in vitro* measurements (total plasma concentrations, total brain concentrations, PPB, and brain tissue binding). For comparing and prioritizing key compounds, one might like to consider generating multiple $K_{p,uu}$ data points (e.g., $n = 2$) to increase confidence in the $K_{p,uu}$ values.

2.2. Experimental Methods Commonly Used To Measure or Estimate Brain Exposure. Microdialysis is the

method of choice for the direct measurement of unbound drug concentrations ($C_{u,b}$) within the brain ISF.²⁸ This powerful technique enables investigations into the extent as well as the rate of drug delivery to the brain, providing critical parameters for PK/PD modeling. However, similar to RO studies, technical challenges and resource requirements limit its use in drug discovery to more advanced drug candidates.

CSF sampling is a less demanding and therefore more widely employed technique for assessing brain exposure during early drug discovery. The CSF is separated from the ISF compartment by only a single layer of ependyma, a cell layer that does not have tight junctions. Due to the very low protein levels in CSF, approximately 0.2 mg/mL compared to 70 mg/mL in plasma, drug CSF concentrations (C_{CSF}) can be approximated by $C_{u,b}$. Indeed, microdialysis studies of brain distribution, as well as PK/PD studies for a range of preclinically and clinically used compounds, suggest that the drug CSF level is generally a good approximation of the brain ISF concentration.³⁷ A comparative study of brain exposure in rats for 39 structurally diverse drugs demonstrated a 3-fold agreement between drugs with respect to $K_{p,uu}$ (ISF) and $K_{p,uu}$ (CSF), within a similar rank order.³⁸ However, one should remember that the CSF approximation fails for compounds that are subject to active efflux or influx ($K_{p,uu} \ll 1$ or $\gg 1$), presumably due to the lower active transport capacity of the blood–cerebrospinal fluid barrier compared with that of the blood–brain barrier.³⁹ For example, while the C_{CSF} significantly overpredicts the $C_{b,u}$ of highly effluxed drugs, such as loperamide, it underpredicts the $C_{b,u}$ of actively influxed drugs, such as oxycodone.³⁸

CSF sampling has a high value in CNS translational studies, being the only generally applicable method of obtaining information on free drug concentrations in the human brain.⁴⁰ Studies comparing rat and human CSF data showed that the human $K_{p,uu}$ (CSF) was, on average, approximately 3-fold higher than the rat $K_{p,uu}$ (CSF).³⁸ Some of the proposed explanations for the observed species difference include the disease state of the patients (e.g., altered BBB function), active transport, kinetic bias due to timing of CSF sampling, and the different sampling site (cisterna magna in the rat vs lumbar puncture in the patients).³⁸ In any case, the 3-fold error is generally considered to be of little pharmacokinetic or pharmacodynamic consequence for the prediction of drug concentrations in human CSF on the basis of rat CSF concentrations. However, prediction of rat unbound brain exposure based on rat CSF concentration includes an additional 3-fold error, which results in a cumulative 9-fold error margin in prediction of human $C_{u,b}$ solely on the basis of rat CSF exposure.⁴¹ This may have significant consequences if a drug has a narrow therapeutic window. In order to enhance the predictive power of modeling human $C_{u,b}$ and related PK/PD relationships on the basis of preclinical data, more complex physiologically based PK (PBPK) algorithms have been developed in recent years, which also incorporate mechanistically relevant *in vitro* data and integrate drug-dependent physiological and biological parameters, as they vary between species, subjects, age, or disease state.^{41,70}

A more screening-based approach commonly used in early drug discovery due to much higher throughput is the brain homogenate-based estimation of unbound drug concentrations in the brain ($C_{u,b}$). This method relies on a combination of the *in vitro* measured fraction unbound in the brain ($f_{u,b}$) and the relatively straightforward *in vivo* determined brain total concentration (C_b). The $f_{u,b}$ data are generated in a high-throughput fashion using a simple and elegant method based

on the equilibrium dialysis of compounds between brain homogenate and buffer, which is used to calculate the unbound concentration in the brain ($C_{u,b} = f_{u,b} \times C_b$).⁴² An alternative to the *in vitro* $f_{u,b}$ determination method preserves the cellular structure of the brain tissue using brain slices.⁴³ In contrast to the brain homogenate method, this approach can capture potential differences between ISF and intracellular fluid (ICF) drug concentrations, as observed for gabapentin.³⁵ Since this phenomenon is thought to be relatively rare, generally associated with compounds that are actively transported into tissue, the more elaborate slice method is considered mainly when other techniques fail to explain the PK/PD relationship.

It is important to note that due to a very poor correlation the free fraction in plasma ($f_{u,p}$) is not a suitable surrogate for $f_{u,b}$.⁴⁴ This lack of correlation is mostly a consequence of the very different lipid and protein contents of the two compartments, with plasma having twice as much protein and the brain having 20-fold more lipids.²⁸ However, the free drug hypothesis infers that at steady state, irrespective of differences in $f_{u,p}$ and $f_{u,tissue}$, the unbound drug concentration in the tissue of interest is mirrored by $C_{u,p}$, i.e., $C_{u,plasma} = C_{u,tissue}$. For example, following either single or multiple doses of the antifungal drug fluconazole, similar free drug concentrations are found in a range of body fluids, including plasma, CSF, saliva, breast milk, vaginal secretions, sputum, and prostatic and seminal vesicle fluid.⁴⁵

Species dependence of plasma protein binding is a well-documented phenomenon. Summerfield and colleagues at GlaxoSmithKline reported marked variations on comparing human $f_{u,p}$ values with rat ($R^2 = 0.49$) and pig ($R^2 = 0.65$) for a set of 21 CNS drugs and PET tracers.⁴⁶ This is hardly surprising considering the evolutionary divergence in the structure of blood proteins and overall blood content. In contrast, however, Summerfield et al. found good interspecies correlations for $f_{u,b}$ values among rat, pig, and human ($R^2 > 0.9$; $n = 21$).⁴⁶ Similarly high degrees of $f_{u,b}$ correlation were reported by Di et al. at Pfizer for a set of 47 drugs in six different species and in two different strains of rat.⁴⁷ This evidence supports the commonly accepted practice of using rodent $f_{u,b}$ values in human PK prediction models. It was suggested that interspecies similarities in $f_{u,b}$ reflect the conserved brain general morphology across species and mainly nonspecific nature of drug binding to brain lipids, since the brain-lipid content is higher than that in plasma and protein binding within brain tissue is thought to be insignificant.⁴⁸ Therefore, if species differences in brain exposure of passively diffused drugs are observed, then they are likely to be driven by differences in plasma protein binding where the homology varies significantly from one species to another.

Plasma protein and brain tissue binding are clearly very important parameters for understanding drug PK, PD, and safety properties. However, theoretical analyses and experimental observations suggest that these parameters should not be the primary focus of optimization efforts in drug discovery.^{30,49} Indeed, high tissue binding is generally not considered to be a liability, as many successful drugs exhibit low f_w , e.g., 24% of all drugs launched between 2003 and 2013 have PPB > 99%, whereas 15 out of 32 the most prescribed CNS drugs have $f_{u,b} < 5\%$.⁴⁹ It has also been pointed out that lowering brain tissue binding does not necessarily lead to higher $C_{u,b}$ and consequently, instead of focusing on $f_{u,p}$ and $f_{u,b}$, discovery teams should place a stronger emphasis on minimizing intrinsic clearance and BBB efflux transport to achieve high $C_{u,p}$ and $C_{u,b}$.⁴⁹ It is worth noting that improved $C_{u,p}$ and $C_{u,b}$ levels,

especially when achieved by reducing lipophilicity, are often accompanied by increased unbound concentrations (e.g., Tables 3 and 4). Ultimately, assuming all other properties being equal, one may still prefer drugs with higher f_u levels, which may translate into lower daily dose requirements.

2.3. BBB Permeability and Active Transport. A fine interplay between passive membrane permeability and active transport processes at the BBB level, together with plasma/brain tissue binding, is widely recognized as being the primary determinant of drug disposition within the CNS. However, despite decades of experience in culturing brain endothelial cells, there is still no satisfactory *in vitro* model of the BBB available to date. Culturing primary brain endothelial cells is too difficult for routine applications, whereas immortalized brain endothelial cell lines lack the required junction tightness. Still, useful high-throughput permeability assays have been developed using alternative cell lines, such as Caco2 (heterogeneous human epithelial colorectal adenocarcinoma cells), porcine kidney (LLC-PK1), and the industry favorite MDCK (Madin–Darby canine kidney) cell lines.⁵⁰ Although these cell lines are neither endothelial cells nor do they originate from the brain, the tightness of the monolayer results in permeability values (P_{app}) that correlate well with *in vivo* permeation. Due to its significantly lower cost and higher throughput, a parallel artificial membrane permeability assay (PAMPA)⁵¹ that lacks transporter proteins can be positioned in a screening flow scheme to remove poorly permeable compounds from testing in the MDCK cell line.

Active efflux and poor permeability tend to exert a much greater effect on CNS than peripheral exposure, mainly because the transporters at the BBB are less likely to be saturated, as the drug concentration in the brain blood capillaries is much lower than that in the gut. Consequently, the physicochemical property requirements for brain exposure are generally more stringent. In a comparative study of marketed CNS and non-CNS drugs examined using MDCK assays, 96% of the CNS drugs exhibited passive permeability (P_{app}) greater than 150 nm/s, whereas only 76% of the non-CNS drugs met this criterion.²⁸ On the basis of these results, a widely quoted $P_{app} > 150$ –200 nm/s cutoff was suggested for compounds designed for CNS targets. In contrast, a lower threshold value of $P_{app} > 100$ nm/s is the generally accepted guideline for achieving good oral bioavailability.⁵²

Limited brain exposure due to active efflux is a common issue for CNS drug discovery programs. Among the transporters known to be expressed in BBB endothelial cells that can affect drug transport in either direction,⁵³ P-glycoprotein (P-gp, or MDR1), an active efflux transporter, is by far the most studied and best understood.⁵⁴ This large transmembrane glycoprotein, first discovered in mutant cancer cells that appeared to alter membrane permeability for chemotherapeutics, belongs to the ATP-binding cassette transporter superfamily, which uses the energy of ATP hydrolysis to extrude compounds across a lipid membrane (hence named permeability glycoprotein, P-gp).⁵⁵ This was a ground breaking discovery, providing a rationale for a frequently observed cancer treatment failure due to resistance to multiple chemotherapeutics. Years later, P-gp was found in the brain, expressed at high levels at the luminal face (blood-side) of the brain vascular endothelium, in addition to the endothelial cells of the choroid plexus, where it facilitates transport toward the CSF.⁵⁶ In fact, P-gp has been found widely expressed in a variety of tissues, including the intestine, liver, kidney, testis, and placenta.⁵³ Interestingly, CNS drugs were found to have a

significantly lower incidence of P-gp-mediated efflux than non-CNS drugs, suggesting the greater importance of P-gp efflux for CNS therapeutics.⁵⁷ This is probably because, in contrast to the intestine, drug plasma concentrations at the BBB can rarely reach P-gp saturation levels.

In humans, P-gp is encoded by a single gene (MDR1), whereas in rodents, there are two genes, *mdr1a* and *mdr1b*. They are both expressed in brain; however, only *mdr1a* is found at the BBB, whereas *mdr1b* is expressed in brain parenchyma.⁵⁸ The significant species-dependent substrate recognition divergence is a relatively rare occurrence,^{54,59} although compounds that exhibit difference between rodent and human efflux ratios have been observed.⁶⁰ These observations are consistent with a relatively high primary sequence homology between human and rodent P-gp transporters, also shared with other species, e.g., there is 85–93% sequence homology among human, mouse, rat, dog, and rhesus monkey.⁵⁹

The continuous research focus on P-gp is a reflection of its apparent role as the main BBB gatekeeper with the broadest substrate specificity. Its molecular recognition promiscuity is better understood since the recent publication of the mouse P-gp apo crystal structure at 3.8 Å resolution, along with two co-crystal structures with the enantiomers of a P-gp inhibitor, which revealed an internal cavity of ~ 6000 Å³ with a very large hydrophobic substrate binding site and two ATP-binding domains.⁶¹ The crystal structures support a “hydrophobic vacuum cleaner”⁵⁴ model whereby the substrate partitioned from the outside of the cell into the membrane bilayer enters the P-gp binding pocket through an open portal at the level of the inner leaflet of the lipid bilayer. With the substrate in place, ATP binds to the two nucleotide binding domains, triggering a large conformational change that presents the substrate to the extracellular space while occluding the cytosolic side, thereby providing unidirectional transport to the outside. ATP hydrolysis and dissociation returns the protein to its inward facing conformation, ready for the next transport cycle. The proposed transport mechanism is also consistent with the observation that increasing passive permeability is often accompanied by a lower likelihood of P-gp efflux.⁶² It is possible that compounds that rapidly diffuse across the membrane could overwhelm the P-gp efflux process and, to some extent, escape into the cytosol. Therefore, increasing passive permeability can be seen as a potential strategy for addressing the risk of efflux by P-gp.⁶³

Two decades after the discovery of P-gp, another member of the ATP-binding cassette transporter superfamily implicated in cancer multidrug resistance was identified, first in the multidrug-resistant human breast cancer cell line (hence the name breast cancer resistance protein, or BCRP)⁶⁴ and then found widely expressed in tissues including gastrointestinal tract, liver, and kidney, as well as the luminal membrane of the brain capillaries.⁶⁵ Studies using BCRP and the dual P-gp/BCRP knockout mouse point toward BCRP and P-gp having synergistic and potentially compensatory roles in brain exclusion of cancer drugs such as dasatanib⁶⁶ and sunitinib.⁶⁷ On the basis of the currently available structure–activity relationship, an amino-heteroaromatic motif is suggested to be an important substrate recognition element for BCRP.⁵³ However, the relative contribution of BCRP to overall drug BBB efflux capacity, and its broader impact on brain exposure of therapeutic agents outside oncology, is still unclear.^{68,69} Other well-characterized members of the ABC transporter superfamily, such as multidrug resistant protein 1 (MRP1), MRP4, and MRP5, are also found to be expressed in

brain endothelial capillary cells, albeit at lower levels than that of P-gp.⁵³

Similarly to P-gp, BCRP shares high sequence homology across species, e.g., there is 86% homology between human and rat transporters.⁶⁴ However, recent quantitative proteomics studies uncovered a significant interspecies difference in the abundance of these two transporters at the BBB, with P-gp being more abundant at the rat and mouse BBB and BCRP being more abundant at the monkey and human BBB.⁷⁰ Consequently, the incorporation of transporter protein abundances into human brain *in vivo* PK modeling algorithms is considered to be essential for interspecies translational modeling of drugs that are substrates for these two transporters.⁷¹ This translational challenge, in addition to driving doses higher than necessary, is one of the reasons for a general preference given by CNS drug discovery teams to the development of clinical candidates that are not substrates of active transport. Potential risk of drug–drug interactions (DDI) at the BBB has been another frequently raised concern about drugs that undergo P-gp and/or BCRP efflux,⁷² although the extent of this risk has been questioned recently. Following evaluation of clinical evidence, the International Transporter Consortium (ITC) concluded that, while increased CNS distribution of efflux transport substrates has been commonly observed in animal models, the overall risk of the BBB active transport-related DDI and consequent safety events is low in humans.⁷³ This was rationalized by the inability of marketed drugs to achieve unbound systemic concentrations sufficient to elicit appreciable changes in CNS drug distribution. Only a few drugs (e.g., cyclosporine, quinine, and quinidine) were found to have potential for P-gp inhibition at therapeutic doses in humans, but, even so, the magnitude of the potential clinical effect would be low (≤ 2 -fold increase in B/P ratio).⁷³

The MDCK cell line is the most favored *in vitro* assay for assessing P-gp efflux and has provided a large amount of the data reported in the literature. The popularity of this cell line is related to its relatively low background expression of endogenous transporters and stable transfection with human MDR1 or rodent *mdr1a* transporter (MDR1-MDCK or *Mdr1a*-MDCK, respectively). The apparent permeability (P_{app}) for this cell line is determined in both directions, apical-to-basolateral (A–B) and basolateral-to-apical (B–A), to calculate the efflux ratio (ER) defined as the ratio of $P_{app(BA)}/P_{app(AB)}$. ER values greater than 3 are generally used to define P-gp substrates.⁶² The *in vivo* effect of P-gp efflux can be evaluated using either *mdr1a*^{-/-} knockout mice^{35,74} or P-gp inhibitors to create chemical P-gp knockouts, which also enables studies in species beyond mice.^{75,76}

While *in vitro* assays offer lower costs and higher throughput than *in vivo* studies, the complexity of bidirectional assays, such as MDR-1 MDCK, prevents screening a large number of compounds, which is often necessary during the early stages of drug discovery. Therefore, *in silico* tools can be useful for identifying potential issues related to P-gp efflux and prioritizing the design, synthesis, and testing of compounds. The availability of large *in vitro* data sets has enabled the development of numerous *in silico* approaches, ranging from simple rules based on physicochemical properties to more complex quantitative structure–activity relationship (QSAR) models. For example, an analysis of an internal MDR-1 MDCK data set of 2000 compounds at Eli Lilly found that molecules with a topological polar surface area (TPSA) $< 60 \text{ \AA}^2$ and calculated most-basic $pK_a < 8.0$ exhibited a much lower likelihood of

being P-gp substrates (94%), whereas over 75% of P-gp substrates had TPSA $> 60 \text{ \AA}^2$ and a calculated $pK_a > 8.0$. The same data set was used to generate a QSAR model that exhibited a robust prediction profile, with positive prediction values (PPV) and negative prediction values (NPV) over 80%.⁷⁷

These findings are consistent with a recently proposed rule of 4 that suggests that compounds with molecular weights < 400 , total numbers of nitrogen and oxygen atoms < 4 , and basic $pK_a < 8$ are unlikely to be P-gp substrates.⁷⁸ Although a number of CNS-active molecules exceed one of these criteria, the rule of 4 is a useful strategy that researchers can apply to reduce P-gp efflux. Indeed, lowering pK_a and reducing the number of heteroatoms, particularly hydrogen-bond donors (HBD), have proved to be effective medicinal chemistry approaches for reducing P-gp efflux, as will be exemplified below.⁵⁴

In contrast to efflux, active uptake can have a positive effect on brain exposure, particularly for compounds with poor passive permeability, such as the previously mentioned gabapentin and L-DOPA.^{34,79} However, in such cases, understanding the transport mechanism and how that mechanism is influenced by the compound structure to inform the optimization process presents a significant challenge. Even if a project is successful in delivering a clinical candidate, concerns related to cross-species and interpatient variability are likely to be raised. For these reasons, the generally preferred optimization strategy for overcoming the poor permeability of small molecule drugs is by addressing inherent passive permeability rather than by exploiting active transport.

3. PHYSICOCHEMICAL PROPERTIES AND BRAIN EXPOSURE RELATIONSHIPS

The landmark study by Lipinski et al.⁸⁰ of the physicochemical properties associated with the oral bioavailability of drugs and advanced clinical candidates, codified in a simple mnemonic known as the rule of 5 (Ro5), was a major milestone in the evolution of medicinal chemistry from a largely trial-and-error effort to the modern scientific endeavor of today that is driven by robust prediction methods. Analogous to the now widely accepted Ro5 in the design of oral drugs, the physicochemical properties needed for brain penetration have been extensively studied by a number of researchers in the attempt to similarly define the characteristics of successful CNS drugs and drug candidates using a variety of approaches. To illustrate the evolution of scientific thought and the current state of the art in this field, a representative selection from this body of work reported in the literature is summarized in chronological order in Table 2 and discussed below in more detail.

Inevitably, the data set choice greatly influences the conclusions drawn from these analyses, which has spawned much debate in the CNS medicinal chemistry community regarding the best methods for evaluating brain exposure. Many studies have been based on the physicochemical properties of marketed CNS drugs. Consequently, their conclusions reflect not only brain penetration but also the overall ADME and toxicological requirements for a successful CNS drug candidate.⁹⁰ Alternatively, researchers have analyzed large *in vitro* BBB permeation data sets (e.g., MDR1-MDCK, Caco-2, PAMPA) or *in vivo* measurements of brain penetration, such as total brain/plasma concentration ratios (K_p or Log BB). It is important to realize that the former approach provides information on the rate of permeation of the BBB, whereas the latter approach provides information on the extent of penetration, which was historically based primarily on the total

Table 2. Evolving CNS Property Space: Summary of Selected Literature Describing the Physicochemical Properties Required for Optimal Brain Exposure^{13,14}

data set	conclusions and recommendations	year, author(s), ref
P-gp ER for 2000 compounds from Eli Lilly collection	Compounds with TPSA < 60 Å ² and pK _a < 8 are less likely to be P-gp substrates.	2013, Desai et al. ⁷⁷
Medicinal chemistry literature review	General guidelines for minimizing P-gp recognition include HBD count < 2 and the TPSA < 90 Å ² (preferably <70 Å ²).	2012, Hitchcock ⁵⁴
317 CNS and 626 non-CNS oral drugs	CNS drug design property profile guidelines: TPSA < 76 Å ² (25–60 Å ²); at least one N atom; <7 (2–4) linear chains outside of rings; <3 (0–1) HBD; 740–970 Å ³ volume; solvent accessible surface of 460–580 Å ² .	2011, Ghose et al. ⁸¹
119 marketed CNS drugs and 108 Pfizer CNS clinical candidates	Median values for marketed CNS drugs: MW 305.3 Da; cLogP 2.8; cLogD 1.7; MW 305.3; PSA 44.8 Å ² ; HBD = 1; and pK _a 8.4.	2010, Wager et al. ^{82,83}
9571 Caco-2 measurements	Passive permeability is influenced by both MW and LogD: guidelines to achieve >50% chance of high permeability for a given MW: for MW 300–350, AZLogD > 1.1; for MW 350–400, AZLogD > 1.7; for MW 400–450, AZLogD > 3.1; for MW 450–500, AZLogD > 3.4.	2009, Waring ⁸⁴
3059 rat CNS LogBB; 1975 P-gp ER; 50 641 PAMPA P _{app} ; and 986 brain tissue binding measurements	↑ cLogP leads to ↑ brain tissue binding. ↑ cLogP leads to ↑ LogBB. ^b For basic, acidic, and zwitterionic molecules, ↑ cLogP leads to ↑ permeability. Suggested optimal cLogP is <3. ↑ MW leads to ↓ P _{app} , ↑ ER, and ↓ LogBB ^b and ↑ brain tissue binding.	2008, Gleeson ⁸⁵
Mouse C _{u,b} data for 1000 compounds from Eli Lilly collection	Compounds with cLogP < 4 and TPSA 40–80 Å ² are more likely to achieve higher C _{u,b} . ^a	2006, Raub et al. ⁶³
Medicinal chemistry literature review	Suggested physicochemical property ranges for increasing the potential for BBB penetration: PSA < 90 Å ² ; HBD < 3; cLogP 2–5; cLogD (pH 7.4) 2–5; MW < 500. ^a	2006, Hitchcock and Pennington ¹⁵
Marketed CNS drugs	Attributes of a successful CNS drug candidate: MW < 450; cLogP < 5; HBD < 3; HBA < 7; RB < 8; H-bonds < 8; pK _a 7.5–10.5; PSA < 60–70 Å ² .	2005, Pajouhesh and Lenz ⁸⁶
329 launched oral drugs from the period 1983–2002	CNS drugs have significantly different properties relative to non-CNS drugs. CNS drug properties (mean/median): MW (310/307); O + N (4.32/4); HBA (2.12/2); RB (4.7/4.5).	2004, Leeson and Davis ⁸⁷
1000 P-gp measurements	Proposed cut-offs to avoid P-gp efflux liability: MW < 400; N + O < 4; pK _a < 8.	2003, Petrauskas et al. ⁷⁸
Literature review	Rule of thumb for brain uptake: compound with O + N < 5 (~70 Å ²), or cLogP – (O + N) > 0 has a better chance of brain penetration. ^b	2002, Norinder and Haerberlein ⁸⁸
48 CNS and 45 non-CNS drugs	Physicochemical properties of non-CNS drugs differ significantly from CNS drugs, which have ↑ cLogP (CNS mean 3.43); ↑ cLogD (CNS mean 2.08); ↓ HBD (CNS mean 0.67); ↓ PSA (CNS mean 40.5 Å ²).	2002, Polli et al. ⁵⁷
776 CNS and 1590 non-CNS oral drugs that reached at least Phase II	Upper PSA limit for the most of CNS drugs is <60–70 Å ² ; oral drugs do not exceed PSA of 120 Å ² .	1999, Kelder et al. ⁸⁹
125 CNS and non-CNS drugs	PSA can be used as a drugs H-bond capacity descriptor. Improved chance of CNS penetration if MW <450; PSA <90 Å ² , and LogD 1–4.	1998, Van der Waterbeemd et al. ⁹⁰
Young's data set	LogBB ^b can be predicted using LogP alkane/water and calculated molar volume or PSA.	1992, Van der Waterbeemd and Kansy ⁹¹
20 CNS penetrant histamine H ₂ antagonists	LogBB ^b can be increased by ↑ lipophilicity (LogP) or/and reducing hydrogen-bonding capacity.	1988, Young et al. ⁹²
201 barbiturates with preclinical <i>in vivo</i> efficacy data	LogP is critical for <i>in vivo</i> activity. Found drug <i>in vivo</i> efficacy in a parabolic dependence on LogP. Suggested optimal LogP = 2.	1971, Hansch et al. ⁹³

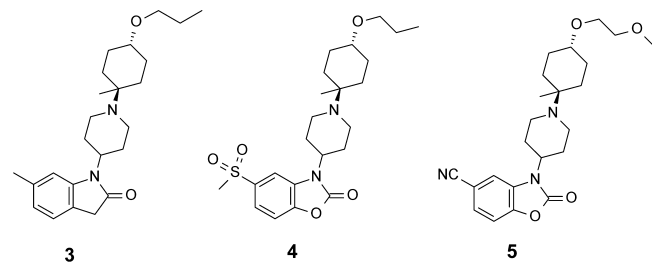
^aBased on drug unbound (free) blood/brain concentrations. ^bBased on drug total blood/brain concentrations; MW: molecular weight; PSA: polar surface area; TPSA: topological polar surface area; HBD: hydrogen-bond donors; HBA: hydrogen-bond acceptors; RB: rotatable bonds; ER: efflux ratio; ↑: increased; ↓: decreased.

drug concentration in the brain. Used in isolation, neither technique provides insight into the more relevant brain free drug concentration (C_{u,b}); therefore, the associated physicochemical guidelines should be interpreted with care.

Understanding how physicochemical properties affect each of the parameters discussed above and how they influence each other enables the design of molecules with optimal CNS exposure. Several physicochemical properties have consistently been found to be important in the context of designing molecules for optimal brain exposure, including lipophilicity, as expressed by calculated logarithm of the octanol/water partition coefficient (cLogP) or calculated logarithm of the octanol/water partition coefficient at physiological pH 7.4 (cLogD), the number of hydrogen-bond donors (HBD) and acceptors (HBA), polar surface area (PSA), ionization state (pK_a), rotatable bond (RB) count, and molecular weight (MW).^{82–87}

One of the critical challenges for the medicinal chemist in drug discovery is balancing multiple physicochemical parameters with SAR to address deficits in one property without negatively

affecting another. For example, increasing lipophilicity can improve BBB permeability, but it may also negatively impact blood clearance and increase nonspecific binding, leading to an overall reduction in C_{u,b}. To achieve an optimal balance, one should have a good understanding of how individual physicochemical properties may influence each other as well as the extent of CNS penetration and the rate of permeation. This Perspective presents a synopsis of recent studies published in the medicinal chemistry literature and attempts to capture the most prominent physicochemical guidelines that have been reported as useful aids for decision making during lead optimization. Key physicochemical properties are discussed sequentially, and their impact on CNS exposure is illustrated with literature examples. However, it should be noted that it is not possible to alter one parameter in isolation, which may confound the interpretation of the controlling factor mitigating CNS exposure. Therefore, the categorization applied here is best regarded as a mnemonic rather than as a rigorous classification.

Table 3. M1 Agonists: Reducing Lipophilicity To Improve $C_{u,b}$ ⁹⁶


compd	M ₁ pEC ₅₀	cLogP	Cl ^a (mL/min/kg)	K _p	f _{u,b} (%)	f _{u,p} (%)	C _{u,b} ^a (nM)	C _{u,p} ^a (nM)	K _{p,uu}
3	9.3	3.5	85	5.7	6	20	2.5	2.6	0.96
4	8.6	1.5	11	0.8	36	40	168	378	0.44
5	8.0	1.5	23	1.7	39	38	261	265	0.98

^a3 mg/kg p.o. (rat).

3.1. Lipophilicity. Lipophilicity is generally regarded to be one of the most important, if not the most important, physicochemical properties, which is critical to control for ultimate success in drug discovery and development. Increasing ligand lipophilicity often results in improved *in vitro* potency, which makes it a relatively straightforward and tempting optimization strategy. However, it is now widely accepted that increased lipophilicity is also accompanied by increased risk of poor solubility and metabolic stability, as well as a greater probability of nonspecific, off-target activities with related toxicological outcomes.⁹⁴

Lipophilicity was the first molecular descriptor to be identified as an important determinant of CNS exposure, including both the rate and extent of drug distribution into the brain. In the 1960s, Hansch et al.⁹³ initiated the field of quantitative structure–activity relationships (QSAR) and, in their early work, demonstrated that the hypnotic activity of around 200 barbiturates depended almost entirely on their lipophilic character, as defined by their octanol–water partition coefficient (LogP).⁹⁵ To minimize the metabolism and side effects, cLogP values of ~2 were suggested to be the most optimal, although it was recognized that a higher lipophilicity may be required to achieve greater CNS efficacy. These observations were later supported by comparative studies of marketed CNS and non-CNS drugs reported by Van de Waterbeemd et al.,⁹⁰ who also introduced a more physiologically relevant lipophilicity indicator: the pH-dependent octanol–water distribution coefficient (LogD). This analysis showed that a good correlation exists between LogD and brain exposure expressed by LogBB, and cLogD values in the range of 1–4 were proposed for optimal LogBB. In comparison, the median cLogD for marketed CNS drugs is 1.7.⁸²

Since both *in vitro* potency and total brain levels are driven mainly by lipophilicity, many CNS drug discovery programs have ended up on a “lipid escalator” with little prospect of success.²⁷ As discussed earlier, the drug discovery reliance on LogBB (based on total brain and plasma concentrations) and its correlation with *in vivo* efficacy, as well as its general pharmacological relevance, have been questioned in recent years.^{16–20,22} In contrast, a good correlation has been found between nonspecific brain tissue binding and cLogP in an analysis of over 3000 diverse compounds from GlaxoSmithKline.⁸⁵ This finding suggests that the higher LogBB values observed for more lipophilic compounds are a consequence of increased nonspecific brain tissue binding, which is unlikely to translate into a therapeutic effect. Importantly,

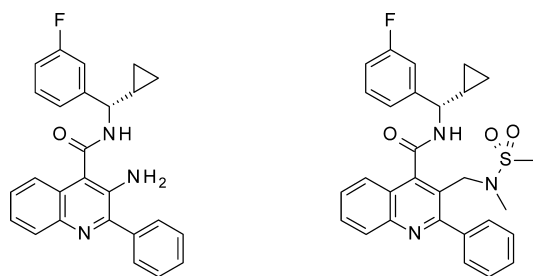
this study also uncovered a negative correlation between $f_{u,b}$ and LogP, which suggests that reducing lipophilicity would be an effective strategy for improving free drug concentrations in the brain and achieving the desired therapeutic profile.

This strategy was adopted by Johnson et al. in their efforts to identify selective muscarinic M₁ agonists for the treatment of the cognitive deficits associated with schizophrenia and Alzheimer’s disease (Table 3).⁹⁶ During the course of the program, a potent and moderately lipophilic oxindole **3** was identified (cLogP = 3.5). Despite a high total B/P ratio (rat K_p = 5.7), its brain unbound drug concentration was very low ($C_{u,b}$ = 2.5 nM), a consequence of higher brain tissue vs plasma protein binding ($f_{u,b}$ = 6% vs $f_{u,p}$ = 20%) and high plasma clearance (Cl = 85 mL/min/kg).

To improve metabolic stability and $C_{u,b}$, a series of analogues with reduced lipophilicity was synthesized, which led to the discovery of benzoxazolinone **4** (cLogP = 1.5). Despite the reduced K_p compared with that of the parent compound **3** (0.8 vs 5.7, respectively), **4** displayed a much improved brain free concentration ($C_{u,b}$ = 168 vs 2.5 nM for **3**), presumably a result of combined improvements in metabolic stability (Cl = 11 mL/min/kg) and brain free fraction ($f_{u,b}$ = 36%). However, an over 2-fold difference between the $C_{u,b}$ and $C_{u,p}$ values ($K_{p,uu}$ = 0.44) suggested that **4** undergoes active efflux, possibly by P-gp, which prevented its further progression. This result led the authors to target additional analogues with a cLogP at ~1.5 but reduced H-bond acceptor capacity, which was thought to be associated with P-gp recognition. This strategy resulted in the identification of nitrile analogue **5** (cLogP = 1.5), which, as a P-gp nonsubstrate ($K_{p,uu}$ = 0.98), achieved an almost 2-fold higher $C_{u,b}$ compared with that of **4** (261 and 168 nM, respectively), despite of its slightly higher clearance in rat (Cl = 23 mL/min/kg). Compound **5** was examined further in PD studies and exhibited a robust pro-cognitive effect in preclinical models at a 1 mg/kg dose.⁹⁶

The optimization of a series of neurokinin-3 (NK₃) receptor antagonists reported by Smith et al. at GlaxoSmithKline is another example that highlights the importance of controlling lipophilicity and looking beyond total brain levels to successfully prosecute CNS optimization programs (Table 4).⁹⁷ Following the first round of optimization of a lead quinolone series, the authors selected two analogues, **6** and **7**, to examine further in an *ex vivo* NK₃ receptor occupancy study in gerbils, which was selected as a suitable species due to its close receptor homology to the human NK₃. *Ex vivo* receptor occupancy

Table 4. NK₃ Antagonists: Total Brain Concentration (C_b) Does Not Correlate with Measured Receptor Occupancy (RO)⁹⁷



6, GSK172981

7, GSK256471

compd	cLogP	hNK ₃ (pKi)	dose ^a (mg/kg) (route)	C _b (nM)	f _{ub} (%)	RO ^b (%)
6	6.8	8.7	30 (ip)	5011	0.7	60
7	4.5	9.0	10 (po)	118	3.3	61

^aGerbil. ^bRO (%) obtained from brain homogenate binding experiment (gerbil).

(RO) was determined using a homogenate binding technique and the cortical tissue harvested following a 1 h pretreatment time. As shown in Table 4, despite the higher whole brain exposure observed for compound 6, its receptor occupancy at 30 mg/kg i.p. was similar to the occupancy observed for compound 7 at 10 mg/kg p.o. Equilibrium dialysis measurements of the brain tissue binding revealed a ~5-fold lower unbound fraction for 6 (cLogP = 6.8) compared with that of the less lipophilic analogue 7 (cLogP = 4.5). This difference, together with the slightly higher affinity of 7 for the NK₃ receptor, offsets the over 40-fold lower total brain concentration of 7 compared with that of 6 (118 nM vs 5011 nM), which results in RO levels that predict equivalent efficacy *in vivo*.

In addition to the extent of drug distribution into the brain, as discussed above, lipophilicity also affects the rate of drug distribution into the brain (BBB permeation). For example, an analysis of over 50 000 data points from a PAMPA assay at GlaxoSmithKline showed that increased LogP is associated with increased passive permeability of molecules containing ionizable groups, such as acidic, basic, or zwitterion groups. Interestingly, no such linear correlation was observed for neutral molecules.⁸⁵ Consistent with these findings, Waring's analysis of a large Caco-2 data set at AstraZeneca indicated that LogD is a better permeability predictor than LogP.⁸⁴ He also demonstrated that, in addition to LogD, molecular size also must be considered. As MW increases, LogD must also increase to maintain a 50% probability of high permeability. For instance, a 300–350 Da compound requires a cLogD > 1.1, but a 450–500 Da compound requires a cLogD > 3.4.^{84,98}

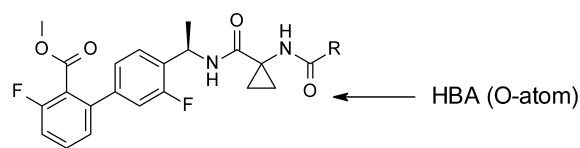
Because permeability is a principal prerequisite for CNS penetration, it is tempting to optimize compounds for a very high permeability using the rapid *in vitro* screens described above. However, if offset by other parameters (e.g., no active efflux, low plasma clearance, or high f_{ub}), even low-to-moderate permeability may suffice. Therefore, optimization efforts should focus on improving K_{p,uu} and C_{ub} since these two parameters have a much greater impact on the desired pharmacological efficacy.²³ The significance of K_{p,uu} is well-reflected by the fact that among CNS-active drugs it varies by a factor of up to 150-fold, whereas the range for log B/P ratios (K_p) differs by up

to 2000-fold, and for BBB permeability, it spans an even larger range of up to 20 000-fold differences.⁹⁸ High permeability is more critical for acute treatments that need fast-acting drugs, e.g., anesthetics or analgesics for acute pain. It is of lesser importance for chronic administration schedules, where even poor permeants can elicit significant pharmacological effects, as seen for morphine-6-glucuronide 2.²⁶

3.2. Hydrogen Bonding. In the context of CNS drug design, H-bonding capacity is probably the most critical physicochemical property due to its effect on a multitude of properties related to brain exposure. Studies using artificial membranes (PAMPA) suggest that increased H-bonding potential is associated with lower passive permeability.⁵² This is related to the desolvation of the associated hydrogen-bound water molecules that is required for membrane permeability as well as lipid solubility. This effect is often further exaggerated in biological membranes, where an increased H-bonding potential also increases the risk of P-gp recognition.⁵⁴ In addition to the rate of permeation, the extent of unbound brain exposure has also been found to be dominated by H-bonding capacity, e.g., removal of two HBAs can lead to a 2-fold increase in K_{p,uu}.³⁸ These findings are consistent with molecular property analyses showing that CNS drugs have significantly lower numbers of H-bond donors (HBD)⁵⁷ and H-bond acceptors (HBA)⁸⁷ compared with that of non-CNS drugs. Consequently, the reduction of H-bond donors and acceptors is often a successful strategy for optimizing the targeting of the CNS. Pajouhesh and Lenz proposed the following frequently quoted guidelines for successful CNS drug candidates: H-bond donors < 3, H-bond acceptors < 7, and total H-bonds < 8.⁸⁶

In many cases, a simple HBD/HBA count could be used to successfully differentiate chemotypes for the relative likelihood of P-gp recognition. However, because not all HBDs and HBAs are equal in terms of the strength of the H-bond they that they can form,⁹⁹ incorporating relative H-bond strength into molecular design can be an effective strategy to reduce P-gp efflux. According to a global model based on Abraham's HBD and HBA strength parameters, α and β , respectively,⁹⁹ compounds with $\beta < 1.7$, MW < 400, and the most basic pK_a < 8 are likely to be nonsubstrates.^{62,78} For example, a set of B₁ receptor (BK₁R) antagonists reported by Kuduk et al.,¹⁰⁰ which differ only in the substitution at the terminal amide group, were found to have similar BK₁R potencies and the same HBD/HBA count and acceptable passive permeability while exhibiting a range of ERs (Table 5).

Table 5. B₁R Antagonists: Lowering HBA Strength To Reduce P-gp ER¹⁰⁰



compd	R	B ₁ R K _i (nM)	HBA ^(O atom) strength ^a	P _{app} ^b (nm/sec)	ER
8	–CH ₃	0.9	2.12	210	8.6
9	–CHF ₂	0.4	1.63	310	3.2
10	–CF ₃	0.6	1.39	280	2.3
11	–CF ₂ CF ₃	1.6	1.35	310	1.4

^aDesai et al.⁶² ^bMDR1-MDCK: passive apparent permeability coefficient with P-gp inhibited.

Table 6. PDE10A Inhibitors: Reducing HBD Capacity To Improve Brain Exposure¹⁰¹

compd	12	13	14	15	16	RO ^c (%)
	PDE10A IC ₅₀ (nM)	HBD	ER ^a	Cl ^b (L/h/kg)	F ^b (%)	
12	92	3	76.7			
13	1.1	2	11.1			
14	4.3	1	2.4			
15	4.5	1	0.9	0.53	10	21.3
16	5.1	1		0.07	56	57.1

^aMDR1-MDCK. ^bFed male Sprague–Dawley rats; dose: 5 mg/kg p.o. ^cDose: 10 mg/kg.

Clearly, the effect of a fluorine substitution in BK₁R on the ER could not be explained by HBD/HBA count or PSA because these values are the same for all analogues. There is also very little difference in their permeabilities, P_{app} 210–310 nm/s. To explain the observed difference in ER, the authors proposed that the strong electron-withdrawing effect of fluorine substitution makes the amide carbonyl group a poorer HBA with consequently reduced P-gp recognition.¹⁰⁰ This hypothesis has been supported by a quantum mechanical HBD/HBA strength calculation reported by Desai et al.,⁶² which found that the HBA strength of the terminal amide carbonyl group dropped approximately 10-fold, from 2.1 to 1.3 (the values are in log scale), as the number of fluorine molecules increased across compounds 8–11 (Table 5).

A reduction in HBD capacity is one of the most frequently reported medicinal chemistry strategies for improving brain exposure. For example, this strategy was employed by Hu and colleagues at Amgen while optimizing the CNS exposure of a benzimidazole series of PDE10A inhibitors that they were developing for the treatment of schizophrenia (Table 6).¹⁰¹

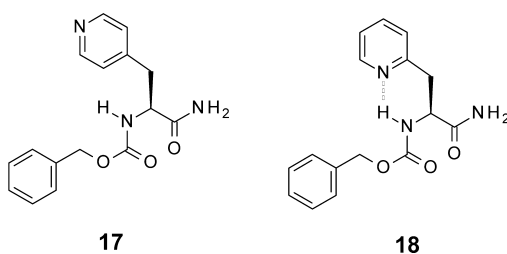
One of the initial leads in the program was compound **12**, a potent and selective PDE10A inhibitor (IC₅₀ = 92 nM), which was also a strong P-gp substrate with an efflux ratio (ER) in the MDR1-MDCK assay of 76.7. Early SAR investigations indicated that the piperidine alcohol moiety in **12** is not critical for potency and can be replaced by groups lacking HBDs. In fact, a morpholine analogue, **13**, displayed almost 2 orders of magnitude higher potency (IC₅₀ = 1.1 nM) with one HBD less than **12** and with a reduced ER of 11.1. Encouraged by these initial results, the authors further pursued the HBD-reduction strategy, which led to the identification of benzothiazole **14**, a slightly less potent PDE10A inhibitor (IC₅₀ = 4.3 nM), but with the P-gp efflux reduced to an acceptable 2.4 ER. Because a co-crystal structure of the HTS hit (**12**) bound to PDE10A suggested that the NH linker was not essential, the authors decided to replace it with a carbonyl group to further reduce the HBD count while maintaining the observed planarity of the phenyl and the benzimidazole rings. The resulting keto

analogue **15** not only retained the low nanomolar PDE10A potency but also exhibited a low efflux ratio of 0.9. The modest target engagement achieved by this compound at 10 mg/kg (RO = 21%) and 30 mg/kg (RO = 55%) in rats (p.o.) was attributed to its poor systemic exposure, which was related to the oxidative metabolism of the morpholine ring. Optimization around that region of the molecule led to the identification of piperazine analogue **16**, which had a superior ADME profile and 57% RO at 10 mg/kg (p.o.).¹⁰¹

A slightly greater impact on the ER of the carbonyl group in **15** compared with that of the benzothiazole in **14** could be rationalized by a masking effect of an intramolecular hydrogen bonding (IMHB) between the carbonyl group and the last remaining HBD in **15** (Table 6). Indeed, the introduction of an IMHB motif can be an attractive alternative to the complete removal of HBD. When a hydrogen-bond donor and acceptor are on the same molecule in close proximity, an equilibrium may exist between closed conformations where an intramolecular hydrogen bond is formed and open conformations where the polar groups are exposed to solvent.¹⁰² The closed forms, masking the polarity from the environment, are likely to be more lipophilic and may consequently display higher membrane permeability, whereas the open forms are more water-soluble.

The incorporation or reposition of an existing HBA in a molecule to enable intramolecular H-bond formation is a widely employed property optimization strategy, particularly when the HBD is required for target activity.⁶² By practically removing polar HBD and HBA groups from the molecular environment, the formation of an IMHB can result in increased lipophilicity, which, in turn, may improve passive permeability as well as impair P-gp recognition, as shown in Table 7.¹⁰³

One important consideration when designing an IMHB is the equilibrium between the open (polar) conformations and the closed (nonpolar) conformation, which is needed to achieve optimally balanced molecular solubility and permeability properties. For example, to improve aqueous solubility, one could consider introducing steric constraints or altering ring size

Table 7. Intramolecular H-Bond (IMHB) Improves P_{app} and ER¹⁰³

compd	HBD	P_{app}^b	ER ^c
17	2	43	3.1
18	2 ^a	177	1.1

^aIncludes one intramolecular H-bond. ^bApparent AB permeability in the MDR1-MDCK assay. ^cBA/AB permeability ratio in the MDR1-MDCK assay.

in the closed form to shift the equilibrium toward the open, more water-soluble conformation. An elegant analysis of the Cambridge Structural Database (CSD) and the Protein Data Bank (PDB) by Kuhn and co-workers suggested a relatively high propensity for intramolecular hydrogen bonds to form five- to eight-membered rings.¹⁰² By far the highest frequency motif was found to have planar, six-membered rings stabilized by conjugation with a π -system. A number of less explored topologies have also been identified, including weaker six-membered ring hydrogen bonds containing one sp^3 center and nonplanar seven- and eight-membered ring topologies.¹⁰²

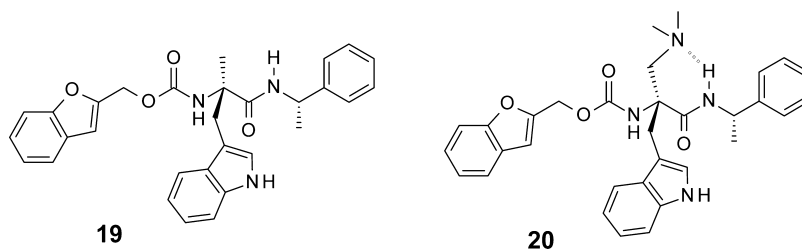
One of the first reported intentional uses of an IMHB designed to improve CNS exposure was in the optimization of a series of NK₁ receptor antagonists described by Ashwood et al.¹⁰⁴ The initial lead **19** (Table 8) displayed a desired pharmacological profile with an oral bioavailability of 60% in dogs and a half-life of greater than 6 h; however, it also exhibited poor solubility (<2 mg/L) and a modest total brain–plasma ratio in rat ($K_p = 0.6$). The authors reasoned that the inclusion of an HBA at the amide alpha-carbon could potentially lead to the formation of an IMHB with one of the neighboring N–H's from the urethane or amide groups. They hoped that the resulting compounds would display improved permeability due to the effective removal of an HBD and HBA in the IMHB as well as increased aqueous solubility. While the inclusion of an NMe₂ group in **20** did not affect NK₁ potency, it did produce a desirable profile with improved solubility and total brain exposure, despite reduced total plasma AUC,

which ultimately resulted in a greatly improved K_p (Table 8). Since $K_{p,uu}$ values were not reported, it is difficult to establish to what extent the improved total brain exposure of compound **20** was driven by the nonspecific tissue binding. However, a significantly higher efficacy of compound **20** in the centrally mediated gerbil foot tapping paradigm with minimum effective dose (MED) of 1 mg/kg is indicative of its superior free brain exposure when compared to that of parent compound **19** (MED = 30 mg/kg).

The enhanced efficacy of **20** was rationalized by a combination of improved solubility and reduced HBD count by IMHB. The presence of an IMHB between the NMe₂ and the amide hydrogen, forming a six-membered ring, has been substantiated by variable-temperature nuclear magnetic resonance (NMR) spectroscopy studies.¹⁰⁴ Although it is likely to be protonated at physiological pH conditions, the amine can pass through lipophilic cell membranes only in its unprotonated form, in which the observed IMHB would increase apparent molecular lipophilicity and consequently cell membrane permeability. A similar amide NH → N₃R IMHB and its impact on molecular properties such as lipophilicity and permeability have been described more recently by Over and colleagues at AstraZeneca.¹⁰⁵

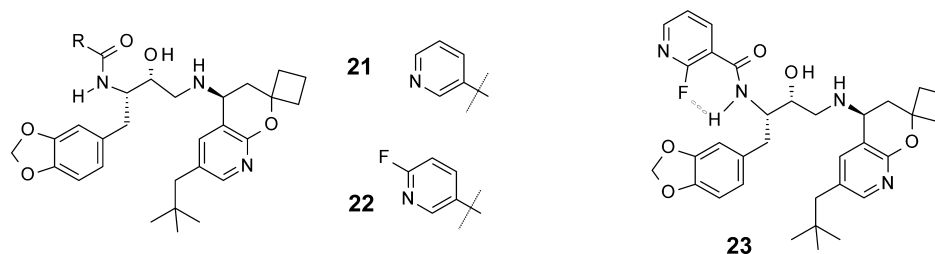
There is a scaffold-dependent limit to which molecular polarity can be increased with the addition of a polar HBA before showing a deleterious effect on membrane penetration, presumably due to a high water desolvation penalty. This issue could potentially be avoided by considering an intramolecular halogen bond, the existence of which has been supported by X-ray crystallography evidence.¹⁰⁶ Although considerably weaker than classical O...H and N...H H-bonds, an improved property profile has been associated with molecules containing an intramolecular halogen bond. This approach was effectively leveraged by researchers at Amgen in their efforts to decrease P-gp recognition in a hydroxyethylamine series of β -amyloid cleaving enzyme-1 (BACE-1) inhibitors represented by pyridine **21** (Table 9).¹⁰⁷

BACE-1, an intensely pursued target in the quest for a disease-modifying treatment for Alzheimer's disease, is an aspartic protease with a characteristically polar and relatively shallow substrate binding site.¹⁰⁸ Consequently, BACE-1 inhibitors are large molecules that are generally characterized by a high PSA and HBD/HBA count, which presents a considerable drug discovery challenge in terms of delivering potent inhibitors with optimal brain exposure capable of achieving the desired *in vivo* efficacy. Pyridine **21**, one of the early leads in Amgen's BACE-1 effort, was prototypical; it displayed high

Table 8. NK₁ Receptor Antagonists: Rationally Designed IMHB To Improve Brain Exposure¹⁰⁴

compd	NK ₁ IC ₅₀ (nM)	HBD	PSA (Å ²)	cLogP	AUC _{0–1h} ^b (ng h/g)	K_p ^c	MED ^d (mg/kg)
19	1.0	3	96	5.5	120	0.4	30
20	0.5	3 ^a	100	5.3	50	6.0	1

^aIncludes one IMHB. ^bDose 0.5 mg/kg, i.v. (rat). ^c $K_{p,uu}$ values were not reported. ^dSubstance P induced foot tapping in the gerbil.

Table 9. BACE-1 Inhibitors: Introducing Intramolecular Halogen Bond To Mask a HBD and Reduce P-gp ER¹⁰⁷

compd	BACE-1 IC ₅₀ (nM)	HBD	PSA (Å ²)	cLogP	P _{app} ^a (10 ⁻⁶ cm/s)	ER ^a
21	26.1	3	96.4	4.3	11	49
22	48.4	3	96.4	4.8	18	35
23	33.2	3	96.4	4.8	17	4

^aMDR1-MDCK cell line.

in vitro potency (IC₅₀ = 26.1 nM) as well as moderate permeability and a very high efflux ratio of 49 in a human MDR1-MDCK assay. As discussed earlier, reducing the number of HBDs would be a sensible mitigation strategy for P-gp efflux, except that both the SAR and crystallographic data indicate that all three HBDs in **21** are critical for binding to BACE-1. In such situations, HBD masking should be considered, and when PSA is already high (as in this case), introduction of intramolecular hydrogen bonding may be the preferred option. Gratifyingly, the incorporation of a fluorine atom into position 2 of the pyridine ring to engage in halogen bonding and mask the amide N–H was successful; analogue **23** exhibited an ER that was an order of magnitude lower than that of the parent compound **21** (ER = 4 vs 49, respectively). Interestingly, 5-fluoropyridine derivative **22**, a regioisomer of **21** that lacks an appropriately positioned fluorine atom to mask the amide N–H, displayed a high potential for efflux (ER = 35). This finding supports the intramolecular halogen bond hypothesis as a rationale for the reduced efflux rate observed for compound **23**.

Most commonly used computational methods for the calculation of physicochemical properties are independent of molecular conformation; consequently, they do not account for the potential existence of internal hydrogen bonds. Therefore, researchers should be cautious when relying only on calculated properties, such as cLogP and PSA. Significant discrepancies between the calculated and experimental properties for molecules with intramolecular hydrogen bonds could account for the unexpectedly good *in vivo* pharmacokinetics displayed by molecules that reside in the Beyond Rule of 5 (BRo5) property space.¹⁰⁹

To experimentally confirm the existence of intramolecular hydrogen bonds, ¹H NMR temperature dependency in lipophilic solvents, such as deuterated chloroform or toluene, is often employed. An exchangeable proton that is involved in a hydrogen-bond interaction is more deshielded (higher δ chemical shift value) than a similar, exchangeable proton that is not hydrogen bonded.¹¹⁰ The temperature coefficient (TC) value determined in these experiments corresponds to the slope of the line obtained by plotting the chemical shift versus the temperature of the experiment; this value is generally negative, and compounds containing intramolecular hydrogen bonds exhibit a less negative TC than compounds unable to form an IMHB.¹¹¹

Shalaeva et al.¹¹² described an experimental method to characterize the intramolecular hydrogen-bond capacity using

$\Delta\log P$, which is defined as the difference in a compound's distribution between a protic (octanol) and an aprotic (toluene) solvent. A potential advantage of the $\Delta\log P$ over the NMR method is that it uses a physiologically more relevant environment that is conducive to IMHB formation. However, similar to the NMR method, the $\Delta\log P$ technique is low-throughput and too laborious for a more extensive evaluation of the impact of intramolecular hydrogen bonds during the early stages of the drug discovery process. Recently, several high-throughput methods for intramolecular hydrogen-bond detection have been reported, including chromatographic methods such as supercritical fluid chromatography, as described by Goetz et al.¹¹³ This technique correlates chromatographic retention with the exposed polarity of a molecule; molecules that can form an intramolecular hydrogen bond can hide their polarity and therefore exhibit lower retention than structurally similar compounds that cannot form an intramolecular hydrogen bond.

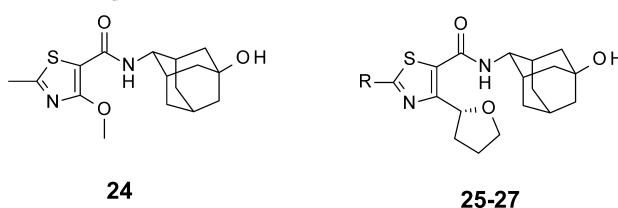
3.3. Polar Surface Area. The polar surface area (PSA) of a molecule is generally defined as the surface area (Å²) over all polar atoms, primarily oxygen and nitrogen, including their attached hydrogens. There are at least three different calculation approaches, each producing considerably different results. The most commonly reported method is the topological polar surface area (TPSA), which is the simplest and therefore the fastest calculation method derived from the 2D atomic connectivity and is independent of molecular conformation. The TPSA is often calculated by the atom-based method, which correlates closely with the total hydrogen-bond count, the sum of hydrogen-bond donors and acceptors.¹¹⁴ A more complex PSA method accounts for the PSA dependence on the conformation and is based on the molecular van der Waals surface of a three-dimensional (3D) conformation. In a simpler version, the method utilizes a single low-energy conformer of the molecule to calculate the PSA, whereas a more sophisticated dynamic PSA calculation includes the Boltzmann weighted average of all conformers within 2.5 kcal mol⁻¹ of the lowest energy conformer found during a conformational search.¹¹⁵ Yet another method calculates the solvent accessible surface area (SASA) by enclosing the water dimension radius of 1.4 Å over a 3D conformation to estimate the polar surface area.¹¹⁶

Often described as a surrogate measure of hydrogen-bonding capacity and molecular polarity, the PSA is a commonly used metric during the optimization of a drug's ability to permeate cell membranes. Molecules with a PSA > 140 Å² generally have

poor gut permeability, leading to low oral bioavailability.⁵² However, reflecting the differences in the gut and BBB permeability as well as plasma and brain tissue binding, PSA values for CNS penetrant compounds tend to be considerably lower. A comparative analysis of marketed CNS and non-CNS drug properties led van de Waterbeemd et al. to propose $PSA < 90 \text{ \AA}^2$ as a cutoff for optimal CNS exposure.⁹⁰ On the basis of a similar analysis of a different data set, Kelder et al. suggested an even more stringent cutoff of $<60\text{--}70 \text{ \AA}^2$.⁸⁹

The optimization efforts around a series of 11β -hydroxysteroid dehydrogenase type 1 (11β -HSD1) inhibitors described by researchers at AstraZeneca provide a good illustration of the impact of the PSA on brain exposure.¹¹⁷ One of early leads in this series, thiazole **24** (Table 10), displayed moderate *in vitro*

Table 10. 11β -HSD1 Inhibitors: Increasing PSA Leads to Reduced $K_{p,uu}$ Values¹¹⁷



compd	R	11β -HSD1 IC ₅₀ (nM)	PSA (\AA^2)	LogD _{7.4}	$K_{p,uu}$ ^a	F ^a (%)
24		61	75	2.0	0.9	23
25	MeO-	7.2	84	2.3	0.7	40
26	cPr(1-CN)CH ₂ O-	22	93	2.6	0.4	79
27	CH ₃ SO ₂ CH ₂ -	486	111	0.4	0.03	65

^aOral bioavailability in male Han Wistar rat at 1 h, 30 mg/kg.

potency (11β -HSD1 IC₅₀ = 69 nM) and favorable physico-chemical properties (e.g., PSA = 61 \AA^2 ; LogD_{7.4} = 2.0), which were translated into modest oral bioavailability and high CNS penetration in rat (F = 12%; $K_{p,uu}$ = 0.9). Further optimization efforts led to the discovery of tetrahydrofuryl analogues such as **25** and **26** with improved *in vitro* potency and rat pharmacokinetic properties when compared to those of lead compound **24**. However, these improvements came at the price of increased PSA, which ultimately impacted the compounds' CNS penetration. Compound **25** with PSA of 84 \AA^2 showed $K_{p,uu}$ of 0.7, whereas **26** with PSA = 93 \AA^2 had $K_{p,uu}$ further reduced to 0.4. This trend continued with sulfone analogue **27** (PSA = 111 \AA^2), which maintained good oral bioavailability

(F = 65%) but had brain exposure at the very limits of analytical detection, with $K_{p,uu}$ value estimated to be as low as 0.03.


Interestingly, despite the reduced CNS penetration, compound **26** ($K_{p,uu}$ = 0.4) achieved a free brain concentration 20-fold over its IC₅₀ at a relatively low dose of 20 mg/kg (p.o.). Because it exhibited the most balanced oral bioavailability and brain exposure in the series, compound **26** was progressed further into preclinical target validation studies to assess the impact of 11β -HSD1 inhibition on body weight and glucose levels in rat.¹¹⁷

Another example illustrating the influence of PSA on CNS exposure is shown in Table 11. Again, the observed poor CNS properties of lead molecule **28** (ER = 5.8; K_p = 0.1) from an Indane series of *R*-amino-3-hydroxyl-5-methyl-4-isoxazolepropionic acid (AMPA) receptor potentiators were attributed to the compound's high PSA (109.1 \AA^2), a consequence of containing two sulphonamide groups.¹¹⁸ Because modifications to the Indane sulphonamide were not tolerated, the PSA optimization efforts were focused on finding alternatives to the less restrictive phenyl sulphonamide moiety. One of the earlier analogues resulting from this study was *N*-methylated analogue **29**, which, consistent with a reduced HBD count, had a lower ER and improved brain exposure (ER = 3.2 and K_p = 0.4).

Seeking further improvements, the authors explored a range of PSA-lowering heterocyclic replacements. This investigation led to the discovery of pyridine analogue **30**, which retained the AMPA potency and cLogP of the parent bis-sulphonamide but significantly reduced the PSA to 67.4 \AA^2 compared with 109.1 \AA^2 for **28**. Accordingly, compound **30** was not a P-gp substrate (ER = 1.1) and exhibited good passive permeability and good brain exposure (K_p = 2.1). On the basis of its favorable overall PK and PD properties, including its efficacy and safety margin in preclinical models, **30** advanced to clinical development for the treatment of cognitive impairment in schizophrenia.¹¹⁸

3.4. pK_a and Ionization State. The majority of CNS drugs contain a basic center. Wager et al. found that a median pK_a value for marketed CNS drugs and Pfizer CNS clinical candidates was 8.4.⁸² There are two schools of thought as to whether this fact reflects an inherent benefit of compound basicity for brain exposure or is merely due to bias in the data set resulting from the fact that many currently prescribed CNS drugs target monoamine receptors or transporters, which ligand pharmacophores contain basic centers. Pajouhesh and Lenz proposed that the optimal pK_a range for CNS drugs is 7.5–10.5.⁸⁶ Although the lower limit of this range would

Table 11. AMPA Positive Allosteric Modulators: Reducing PSA To Improve Brain Exposure¹¹⁸



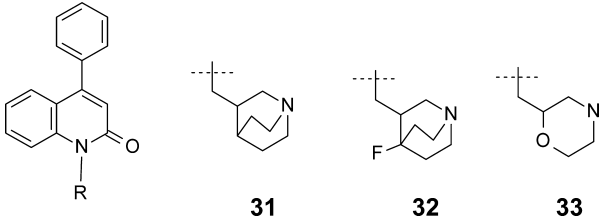
compd	AMPA ^a pEC ₅₀	PSA (\AA^2)	HBD	cLogP	ER ^b	K_p ^c
28	6.1	109.1	2	2.7	5.8	0.1
29	5.9	100.3	1	2.7	3.2	0.4
30	5.6	67.4	1	2.8	1.1	2.1

^aFLIPR-based hGluA₂ flip isoform assay. ^bEfflux ratio in the MDRI-MDCK. ^cBrain–blood AUC_{0–t} ratio (rat).

currently be considered overly conservative, the upper limit is consistent with more recent analyses of P-gp substrate liability (*vide infra*).⁸² In a review of P-gp data for 1000 compounds, Petrauskas proposed a cutoff of $pK_a < 8$ for compounds designed to avoid possible P-gp interactions.⁷⁸

Controlling pK_a was an approach adopted by McDonald et al. at Bristol-Myers Squibb to improve CNS penetration in a quinolone series of $\alpha 7$ nicotinic acetylcholine receptors (nAChR) agonists that they were developing as a potential treatment for the cognitive deficits associated with schizophrenia.¹¹⁹ One of their early leads, quinuclidine 31 (Table 12),

Table 12. $\alpha 7$ nAChR Agonists: Controlling pK_a To Improve Permeability¹¹⁹



compd	$\alpha 7$ nAChR EC ₅₀ μ M	pK_a	ER ^a	P_{app} ^b (nm/s)	K_p ^c
31	0.15	10.1	6.9	900	<0.02
32	5.80	7.6	0.6	380	ND
33	0.26	8.1	1.0	550	0.9

^aCaco-2 $P_{app(BA)}/P_{app(AB)}$. ^bPAMPA, pH 7.4. ^cRat, 30 min.

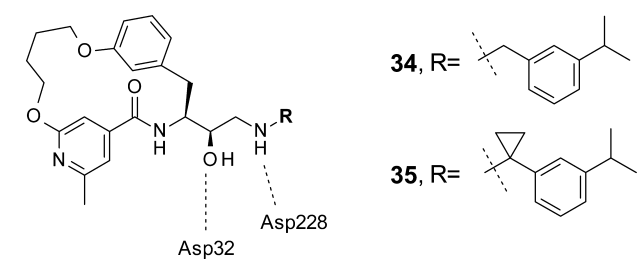
exhibited very poor brain penetration in rats ($K_p < 0.002$), despite its good permeability as measured in a PAMPA assay ($P_{app} = 900$ nm/s). Follow-up experiments revealed that all of the tested quinuclidine analogues in this series exhibited very high efflux ratios in a bidirectional Caco-2 assay, suggesting transporter-mediated efflux.

To test the hypothesis that the observed high ER was related to the quinuclidine high basicity ($pK_a = 10.1$), the authors explored a series of quinolone analogues containing amine groups with reduced pK_a , such as 4-fluoroquinuclidine 32 ($pK_a = 7.6$). Confirming the hypothesis, the less basic compound 32 displayed significantly reduced efflux (ER = 0.6), although the drop in basicity was also accompanied by a substantial loss in $\alpha 7$ activity (EC₅₀ = 5.8 μ M). Gratifyingly, the slightly more basic morpholine analogue 33 ($pK_a = 8.1$) retained $\alpha 7$ potency (EC₅₀ = 260 nM) while displaying near unity ER in the Caco-2 assay, achieving a K_p value of 0.9 in rats at 10 mg/kg dose (no concomitant improvement in $C_{u,b}$ was reported).¹¹⁹

A research group at Novartis employed a similar approach in their efforts to improve the CNS exposure in a series of BACE-1 inhibitors represented by macrocyclic ethanol amine 34 (Table 13).¹²⁰ This initial lead compound was a potent and selective BACE-1 inhibitor; however, it also displayed poor permeability and high efflux in the MDR1-MDCK cell line ($P_{app} = 1.4 \times 10^{-6}$ cm/s; ER = 23). The pK_a -lowering strategy adopted to address these issues required modifications around the ethanolamine group ($pK_a = 8.5$), a critical pharmacophoric element involved in a direct interaction with the catalytic aspartates in the enzyme binding site (Table 13).

Indeed, insertion of small fluorinated alkyl groups such as CHF₂ and CF₃ into the benzylic position next to the amine resulted in improved passive permeability and reduced P-gp

Table 13. BACE-1 Inhibitors: Reducing pK_a To Improve P_{app} and Brain Penetration¹²⁰



compd	BACE-1 IC ₅₀ nM	pK_a	P_{app} ^a (10^{-6} cm/s)	ER ^a	C_b (μ M)	A β 40 ^b (%)
34	32	8.5	1.3	23	0.04	7
35	15	7.3	4.0	3.5	0.32	72

^aMDR1-MDCK. ^bAPP51/16 tg mouse; dose: 60 μ mol/kg.

efflux (data not shown).¹²⁰ Unfortunately, these changes were also accompanied by a complete loss of activity, presumably due to the amine pK_a now being too low for a productive interaction with the catalytic aspartates. A search toward a more tempered pK_a effect led the authors to the design of cyclopropane analogue 35 ($pK_a = 7.3$), which displayed significantly improved passive permeability and reduced ER values ($P_{app} = 4 \times 10^{-6}$ cm/s; ER = 3.5) while retaining high BACE-1 potency. Consequently, this compound showed higher concentrations in the brain (0.32 μ M) and a significantly greater reduction in brain levels of A β 40 (72%) when compared to that of parent benzylamine 34 ($C_b = 0.04$ μ M; A β 40 = 7%). Unfortunately, the introduction of the cyclopropyl group into the ethanolamine motif led to the loss of selectivity over the closely related aspartyl proteases cathepsin D and E, which prevented this series from progressing further.¹²⁰

Contrary to amines, carboxylic acids are generally associated with poor brain exposure due to a combination of multiple factors, including high plasma protein binding, poor passive permeability, and P-gp recognition.⁵³ This trend was first observed in studies related to terfenadine (36, Figure 2),

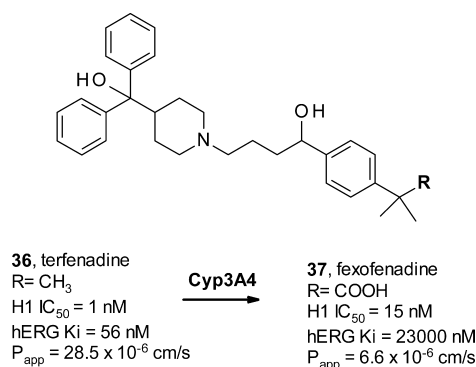


Figure 2. Terfenadine and its main metabolite, fexofenadine.¹²¹

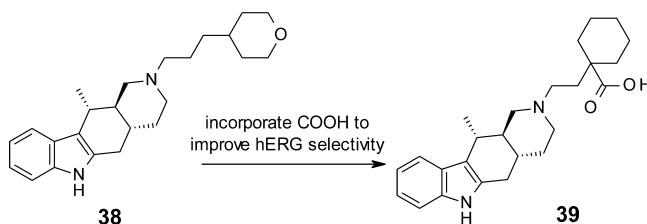
a first-generation antihistamine discontinued in 1997 due to instances of *torsades de pointes*, a polymorphic ventricular tachycardia that can persist and possibly degenerate into a life-threatening ventricular fibrillation.

The cardiac arrhythmia was later associated with a block of a cardiac potassium channel, a product of the human ether- α -go-go related gene (hERG). It was subsequently found that its principle metabolite, carboxylate 37, accounts not only for most

of terfenadine's therapeutic effect but also produced significantly less of the CNS side effects such as sedation as well as a greatly improved selectivity over hERG.¹²¹ On the basis of these findings, the metabolite was subsequently marketed as fexofenadine, the progenitor of the second generation antihistamines that are characterized by a lack of the central side effects intrinsic to the prior generation. The improved CNS side-effect profile of fexofenadine has been attributed to its low brain exposure. Terfenadine has a high passive permeability ($P_{app} = 28.5 \times 10^{-6}$ cm/s) and does not exhibit markedly different brain uptakes in wild type and *mdr1* KO mice. In contrast, zwitterionic fexofenadine has low passive permeability ($P_{app} = 6.6 \times 10^{-6}$ cm/s) and *in vivo* efflux ratio of ~ 50 , as indicated by the *mdr1* KO studies.^{122,123}

Although zwitterions are generally associated with poor CNS exposure, examples of brain-penetrant zwitterionic molecules have been reported in the literature, such as a series of melanin-concentrating hormone receptor-1 (MCHR-1) antagonists described by Mihalic and colleagues at Amgen.¹²⁴ Progress in this intensely pursued research field toward the treatment of obesity and mood disorders has been severely hampered by an extensive MCHR-1 and hERG pharmacophore overlap and consequent cardiovascular risks.¹²⁵ Inevitably, achieving sufficient selectivity over hERG was one of the major challenges faced by the Amgen group, too. An initial lead in their series, compound **38**, was a potent MCHR-1 antagonist with good brain exposure and overall ADME profile and demonstrated efficacy in reducing food consumption in mice (Table 14).

Table 14. MCHR-1 Antagonists: Zwitterions Can Be Brain-Penetrant¹²⁴



compd	MCHR-1 IC ₅₀ (nM)	hERG ^a IC ₅₀ (μM)	Cl ^b (L/h/kg)	K _p	C _{CSF} /C _p	C _b (μM)
38	1	0.03	0.2			0.04
39	0.6	>5	0.55	0.4	0.21	0.32

^aRb⁺ efflux. ^bAPP51/16 tg mouse; dose: 60 μmol/kg.

However, this compound was subsequently found to be a potent hERG blocker, which ultimately prevented its further development. In order to address this issue, the authors considered incorporation of a carboxylic group into the molecule, a strategy commonly employed to improve selectivity over hERG ever since the terfenadine–fexofenadine example was reported.¹²⁶

The hERG evolved, as a potassium cation channel, to stabilize positive charge within its central cavity, which not only may explain why many hERG blockers contain basic amine groups but also rationalize the fact that the presence of a functionality that is negatively charged at physiological pH, such as a carboxylic group, is often detrimental to hERG binding. Indeed, while the replacement of the tetrahydropyran in **38** with a cyclohexyl carboxyl group in **39** did not affect MCHR-1 potency, it resulted in the near complete elimination of hERG potency (IC₅₀ > 5 μM). Importantly, compound **39** (AMG 076) displayed sufficient CNS exposure ($C_{CSF}/C_p = 0.21$;

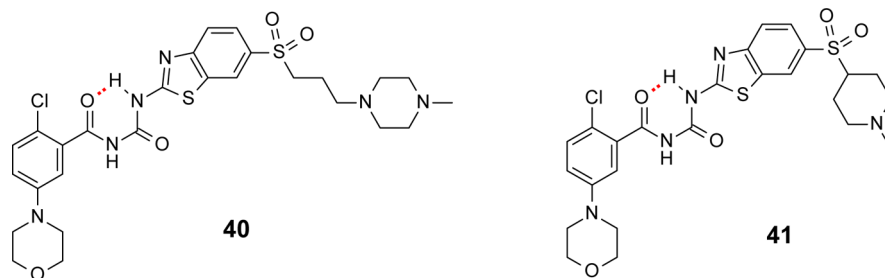
10 mg/kg, p.o.) to produce robust *in vivo* efficacy in mouse models of obesity ($C_{CSF}/C_p = 0.21$; 10 mg/kg, p.o.) and was advanced into the clinic.¹²⁴ A similar zwitterion approach to improve general selectivity profile was successfully employed in the design of brain-penetrant dual H₁/5-HT_{2A} antagonists that advanced into the clinical development for the treatment of sleep disorders.¹²⁷

3.5. Molecular Flexibility and Rotational Bonds. Veber and colleagues at GlaxoSmithKline highlighted the importance of molecular flexibility, as measured by the number of rotational bonds (RB), for predicting rat oral bioavailability and permeation rates in an artificial membrane permeation assay.⁵² They showed that increased molecular flexibility exerted a negative effect on passive permeation. Consistent with the supposition that such effects would have a more profound influence at the BBB, Leeson and Davis demonstrated that the average rotational bond count of oral CNS drugs (mean 4.7, median 4.5) within a data set of oral drugs (1983–2002 NCE list) was reduced relative to the global average across all therapeutic areas (mean 6.4, median 6).⁸⁷ This finding led to the proposed guideline of a rotatable bond count < 8 as an attribute of a successful CNS drug candidate.⁸⁶

The inverse agonist of growth hormone secretagogue receptor type 1a (GSH-R1) **40** reported by scientists at AstraZeneca was characterized by several physicochemical parameters lying outside the range usually associated with good CNS exposure, including high MW (621.2 Da) and PSA (132 Å²) and eight rotatable bonds (Table 15).¹²⁸ Therefore, it was no surprise to find that compound **40** showed no detectable levels in the brain, despite good oral exposure in rats (F = 50%). This result was attributed to a combination of poor permeability and high efflux ratio in the MDRI-MDCK assay, 0.5×10^{-6} cm/s and 69, respectively.

The authors noted that a single-crystal structure of **40** confirmed the existence of an internal hydrogen bond between the urea NH and the amide CO groups, as marked in Table 15. It was reasoned that this intramolecular H-bond effectively masks the physicochemical parameters driven by the acylurea portion of the molecule, e.g., polarity, number of hydrogen-bond donors and acceptors, and RB count. With these considerations in mind, the authors focused their optimization efforts on the flexible side chain region of the molecule to further reduce the number of RBs. This strategy led to the discovery of piperidine **41**, whose physicochemical properties, other than RB count, remained largely unchanged from those of the parent compound **40**. Gratifyingly, this physicochemical profile did translate into significantly improved MDRI-MDCK permeability and efflux, which ultimately resulted in greatly improved $K_{p,uu}$ (0.4) and a free brain exposure multiple of 0.4 ($C_{b,uu}$ divided by IC₅₀ GHS-R1a) in rat at 50 mg/kg. The authors were interested in inverse agonists or antagonists of GSH-R1 as a potential approach to the treatment of obesity; these two compounds enabled them to demonstrate that CNS exposure was necessary to obtain reduced food intake in mice.¹²⁸

Johnson and colleagues at Pfizer recently described their efforts towards CNS-penetrant inhibitors of anaplastic lymphoma kinase (ALK) for the treatment of nonsmall cell lung carcinoma (NSCLC).⁶ NSCLC commonly metastasises in the brain where the current standards of care have only limited effectiveness.⁶ For example, a sample taken at steady state from a single patient at the recommended 250 mg twice daily (bid) dose of crizotinib **42** (Figure 3), approved by FDA in 2011, showed a CSF to free plasma ratio of 0.03 (Table 16).¹²⁹

Table 15. GSH-R1 Antagonists: Reducing Molecular Flexibility (RB count) To Improve Brain Exposure¹²⁸

compd	GSH-R1a IC ₅₀ (nM)	RB count	cLogP	cpK _a (basic)	P _{app} ^a (10 ⁻⁶ cm/s)	ER ^a	K _{p,uu} ^b	free brain multiple ^c
40	0.77	8	1.9	7.8	0.53	69	<0.03 ^c	<0.01
41	6.7	5	2.1	8.1	5.4	2.6	0.42 ^d	0.4

^aA-B MDR1-MDCK. ^b6 h post p.o. dose in rat. ^cDose: 100 mg/kg. ^dDose: 50 mg/kg. ^eC_{u,b}/IC₅₀ (GSH-R1a).

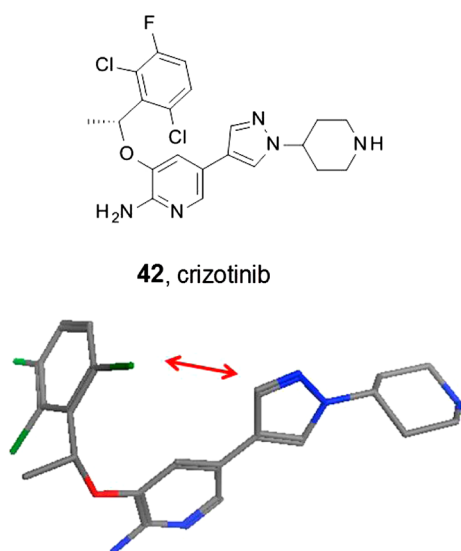


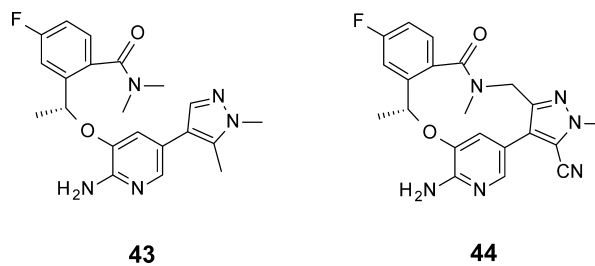
Figure 3. A structure of ALK inhibitor crizotinib, 42, co-crystallized with the ALK kinase domain, PDB 2XP2 (the protein is omitted for clarity).

The lack of CNS exposure can be explained by the compound's high efflux ratio, as measured in the MDR1-MDCK assay. Although early optimization efforts produced leads with improved overall properties, as represented by compound 43,

these improvements were considered to be inadequate, and the team looked for an alternative design approach. Interestingly, the structures of several of these new leads co-crystallized with the ALK kinase domain all showed a typical U-shaped binding conformation, similar to the one observed for 42 (Figure 3), with the aryl and piperazine groups in close proximity.

This observation prompted the authors to consider the synthesis of macrocyclic analogues using the existing amide functionality to connect the two proximal regions of the acyclic template. The macrocycles were expected to reinforce the binding conformation and consequently display improved potency and selectivity profile. In addition, due to the significant reduction in number of RBs and increased buried surface area, the macrocyclics were also anticipated to show improved BBB permeability properties. Indeed, dramatic improvements in all key parameters were observed upon the implementation of this strategy. Amide macrocycle 44 showed over 20-fold higher ALK potency relative to that of acyclic analogue 43 as well as improved permeability and reduced efflux ratio in the MDR1-MDCK assay. Importantly, the AUC ratios of CSF to free plasma of 0.31 suggested that compound 44 is distributed into the CNS. There have been a number of similarly successful examples reported in the literature; consequently, macrocyclization as an approach to improving the molecular properties of drugs has been receiving ever increasing attention in recent years.¹³⁰

3.6. Molecular Weight. CNS drugs tend to be smaller than non-CNS therapeutics. The mean MW of CNS drugs launched

Table 16. ALK Inhibitors: Macrocyclic Analogues Displayed Improved Brain Exposure⁶

compd	ALK K _i (nM)	RB count	PSA	cLogP	P _{app} ^a (10 ⁻⁶ cm/s)	ER	AUC CSF/C _{u,b}
42	0.74	5	78	3.6	12.5	44.5	0.03 ^b
43	22	6	86	2.2	18.8	7.6	
44	0.70	0	110	1.6	28.8	1.5	0.31 ^c

^aA-B MDR1-MDCK. ^bHuman. ^cRat.

between 1983 and 2002 was 310 Da, whereas the mean MW for oral therapeutics (including CNS drugs) was 377 Da.^{82,87} Levin proposed, on the basis of brain capillary permeability measurements in anesthetized rats, that there was a MW cutoff for passive brain permeability somewhere between MW 400–657 Da.¹³¹ Moreover, following an analysis of CNS versus non-CNS drugs, Van de Waterbeemd proposed that the value should be MW < 450 Da.⁹⁰ Waring suggested that the molecular size and LogD are the most critical parameters for predicting permeability in Caco2 cell line: larger molecules require higher LogD to have a chance of high permeability.^{84,98} Of course, molecular weight reduction often has coincidental beneficial effects on other parameters, such as rotatable bonds, PSA, and cLogP, which are, as discussed earlier, frequently employed CNS optimization strategies in their own right. This approach is typically initiated by deletion studies carried out early in hit optimization to establish minimum pharmacophore, which is then optimized while closely monitoring the ligand binding efficiency (LE).¹³²

4. MULTIPARAMETER OPTIMIZATION APPROACHES

As discussed earlier, a good understanding of the general risks and benefits associated with individual physicochemical parameters and their interplay in the context of molecular pharmacokinetic and pharmacodynamics properties is a critical aspect of modern CNS drug design. However, often no single physicochemical parameter can be used to fully explain or predict the intricate pharmacokinetic properties related to brain exposure; rather, more complex multivariate models that interrogate multiple descriptors simultaneously are required.

Waring et al. demonstrated that LogD and MW together predict cell permeability better than LogD alone.⁸⁴ Similar dependencies of BBB permeability on LogD and MW as well as on the PSA and HBD and HBA counts have been reported by other researchers.^{133–135} To simplify the visualization of the multivariate property space and facilitate applications in drug design, there has been a growing interest in the development of scoring functions that combine multiple parameters into a single value. For example, ligand efficiency (LE = $-1.4 \log(K_i [M]) / \text{number of heavy atoms}$),¹³² lipophilic ligand efficiency (LLE = $-\log(K_i [M]) - \text{cLogD}$),⁹⁴ and ligand efficiency-dependent lipophilicity (LELP = cLogP/LE)¹³⁶ are recently introduced scoring functions that normalize the size and lipophilicity contributions to drug potency. While all three efficiency parameters demonstrated utility in hit and lead optimization, only LELP, the multivariate scoring function that combines potency, MW, and cLogP, was found to be able to distinguish marketed drugs from clinical candidates and leads.¹³⁷ Wager et al. reported no significant difference in LE and LLE between 119 CNS drugs and a set of Pfizer's 108 CNS clinical candidates.⁸² The authors reasoned that, given the higher MW and cLogP values associated with the candidate set, the average potency of the compounds in this set must be higher than in the drug set. While the higher MW and cLogP may have contributed to increased potency and favorable LE and LLE values, these properties were also associated with less favorable ADME profiles found in the candidate set. In contrast to LE and LLE, the LELP analysis was able to distinguish drugs from candidates, showing a statistical difference between median LELP values of drugs (5.9) and candidates (7.0).⁸² Similarly, a comparative analysis of a wider range of compounds at different stages of drug discovery, as well as marketed drugs, showed that LELP outperformed LLE for risk assessments

related to ADME and safety properties, further supporting the greater predictive power of multivariate scoring functions.¹³⁷

Wager and colleagues at Pfizer have recently reported an extension of the multiparameter scoring approach into a method designed specifically for CNS drug discovery, termed CNS multiparameter optimization (MPO).⁸³ To assess probability of success, the CNS MPO method utilizes six fundamental molecular parameters: cLogP, cLogD, MW, TPSA, HBD count, and pK_a of the most basic center. Importantly, instead of hard cutoffs, this algorithm constructs desirability scores (0–1) for each of the six properties and composes an overall desirability score using summation, ranging from 0 (undesirable) to 6 (highly desirable). Indeed, an increasing CNS MPO desirability score was shown to align with greater chance of identifying compounds with the desired attributes such as increased passive permeability, reduced P-gp-mediated efflux, and reduced intrinsic clearance of the unbound drug. CNS MPO scores ≥ 4 , as calculated for the majority of CNS active drugs (74%), can be used as a potential reference point when evaluating design ideas.⁸³

In order to further assess the general utility of the CNS MPO algorithm, the author of this Perspective was interested in investigating if the resulting desirability scores could be used to enhance chances of identifying compounds that could achieve high unbound concentrations in the brain ($C_{u,b}$). This is a particularly challenging test, since $C_{u,b}$ is one of the most complex pharmacokinetic parameters, as it is influenced by a multitude of *in vivo* variables, including fraction unbound in the brain, passive permeability, active efflux, and metabolic stability.

For this purpose, the CNS MPO scores were calculated using the published algorithm⁸³ for a diverse set of 616 compounds from Lilly's database with experimental $C_{u,b}$ data. The $C_{u,b}$ values were generated from total brain concentrations measured in the mouse (brain harvested 5 min after a single i.v. dose of 2.17 $\mu\text{mol}/\text{kg}$) and $f_{u,b}$ obtained from the LC/MS analysis of the brain homogenate, as previously reported.⁶³ The compounds were classified, on the basis of their $C_{u,b}$ levels, as low ($C_{u,b} < 10 \text{ nM}$; 44% of the total) and high ($C_{u,b} > 10 \text{ nM}$; 56%). This is an arbitrary classification cutoff used for the purpose of this particular exercise, since the compounds in this set originated from many different programs for which preferred range of the $C_{u,b}$ values would differ greatly. The analysis showed that, at least for this set, the likelihood of finding compounds with high $C_{u,b}$ values progressively increases as the CNS MPO desirability score increases (Figure 4a). For example, 100% of compounds with low CNS MPO scores (≤ 2) had low $C_{u,b}$ values, whereas 81% of compounds with CNS MPO score > 5 had $C_{u,b}$ values classified as high. Although there is still room for improvement, this is a remarkable result considering the challenge presented by the intrinsic complexity of this important pharmacokinetic end point. In contrast, an analysis of the same data set using a single physicochemical parameter, such as cLogD, showed no meaningful alignment, except to note that 86% of the most lipophilic compounds (cLogD > 5) were in the low $C_{u,b}$ group (Figure 4b).

It is therefore not surprising that over recent years MPO methods have been steadily gaining wider acceptance in drug discovery,¹³⁸ with their application to the prospective design of new compounds being particularly appealing. Machine learning algorithms designed to differentiate CNS from non-CNS penetrating compounds on the basis of their substructure fingerprints have also been reported in recent years.¹³⁹ However, these approaches are based on molecular descriptors and fingerprint patterns that are less intuitive and difficult for

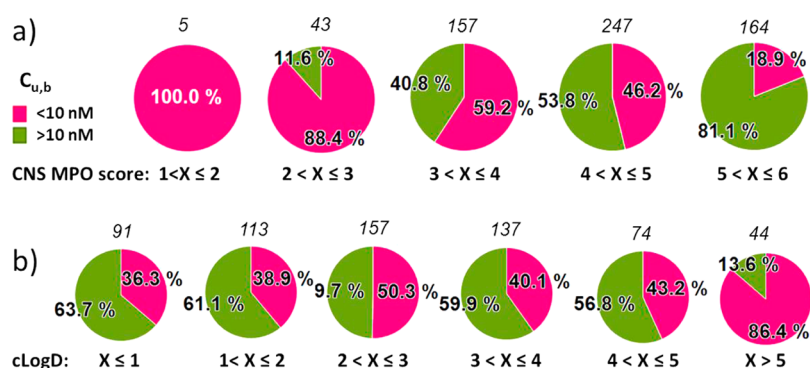


Figure 4. Distribution of brain unbound concentrations ($C_{u,b}$) in mouse for a diverse set of 616 compounds from Eli Lilly's collection as a function of: (a) CNS MPO score (1–6) and (b) cLogD (Chemaxon). Pie charts are colored according to $C_{u,b}$ levels: red, low ($C_{u,b} < 10$ nM); green, high ($C_{u,b} > 10$ nM).

medicinal chemists to translate into optimization hypotheses and desired structural modifications, which may limit their application in prospective design. These algorithms may prove to be more effective when used to select or prioritize structures, for example, to prioritize design ideas for synthesis, to select compounds for focused screening, to triage high-throughput screening (HTS) hits, or to evaluate structures from the patent literature. The MPO algorithms may also prove to be useful in this context.

5. PERSPECTIVES

The existence of the blood–brain barrier presents a unique and major challenge in CNS drug discovery.^{13,14} This challenge can be addressed effectively and successfully only with a good understanding of structure–brain exposure built on reliable and meaningful data. Therefore, it is important to note the large body of evidence described in the literature indicates that total brain concentration (C_b), which is still commonly reported as a measure of brain exposure, is actually a measure of nonspecific binding to brain tissue rather than a pharmacologically relevant concentration. The reliance on drug total brain levels is often misleading, which inevitably and unnecessarily leads to large and highly lipophilic molecules. It is now unambiguously clear that the unbound brain concentration ($C_{u,b}$) is a better measure of drug concentration at the target site and, ultimately, *in vivo* drug efficacy.

As discussed earlier, receptor occupancy (RO) is the most direct measure of target engagement, but the time and cost associated with the required ligand radiolabeling prevent its wider and more impactful application in drug discovery. However, the need for a radiolabeled ligand can be circumvented by a method recently described by scientists at Eli Lilly. They used nonradiolabeled tracers in combination with high-performance liquid chromatography and mass spectrometry (LC/MS) to measure the ROs of several antipsychotics at dopamine D₂ and serotonin 5-HT_{2A} receptors.¹⁴⁰ This method has a potential for a major impact on CNS drug discovery. By eliminating the need for radiolabeled ligands, it enables a routine measurement of *in vivo* RO, which should result in a better understanding of structure–brain exposure at early stages in drug discovery and a more effective execution of hit and lead optimization efforts toward successful drug candidates. Similarly, PET ligand discovery efforts, which focus on radioligand optimization, could also greatly benefit from the LC/MS method. In addition, an elegant extension of the LC/MS detection approach recently reported by Need and colleagues at Eli Lilly

demonstrated the possibility of obtaining reliable RO data simultaneously against multiple targets, thereby establishing ligand selectivity *in vivo* within a single experiment.¹⁴¹

One of the emerging challenges in CNS drug discovery is related to the increasing evidence that mechanisms leading to a failing, more permeable BBB are at the core of the underlying pathology of CNS diseases, such as Alzheimer's disease, multiple sclerosis, ischemic stroke, and injury due to brain trauma.^{11,142} A better understanding of these mechanisms is required to help design more relevant preclinical disease models and therapeutic agents. There is also emerging evidence that the BBB can be altered in certain preclinical models, which may present considerable difficulties when establishing drug PK/PD relationships. For example, a significant increase in P-gp expression has been observed in carrageenan-induced inflammatory hyperalgesia in the rat, resulting in decreased CNS penetration of morphine and the consequent attenuation of morphine-induced antinociception.¹⁴³ Therefore, it is good research practice to use tissues collected from *in vivo* PD experiments for PK studies whenever possible, particularly for the key compounds on which important program decisions are to be made.

One of the fundamental challenges for medicinal chemists working on CNS targets is that the existence of the BBB reduces the size of the CNS drug physicochemical property space compared with the space available to oral drugs designed for peripheral targets. Generally, CNS drugs are smaller, more lipophilic, and have fewer hydrogen-bond donors and lower PSA compared with those of non-CNS drugs.⁸¹ The median values derived from an analysis of marketed CNS drugs offer useful guidance when defining the desirable CNS candidate profile: cLogP = 2.8, cLogD = 1.7, HBD = 1, TPSA = 44.8 Å², pK_a = 8.4, RB = 4.5, and MW = 305.3 Da.⁸² Obviously, these numbers are median values, and there are many marketed drugs with properties at either end of the range. Furthermore, the current CNS pharmacopeia is heavily dominated by drugs that modulate monoamine GPCRs, transporters, and ion channels, many of which were developed for the treatment of psychiatric disorders such as schizophrenia and depression, e.g., out of 118 drugs included in the analysis described above,⁸² 34 are aminergic GPCR ligands, 24 are ion channel blockers, and 11 are aminergic transporter inhibitors. This situation is likely to change, as CNS drug discovery efforts across the pharmaceutical industry have been rapidly refocusing toward emerging CNS therapeutic areas, such as neurodegeneration and oncology. Consequently, there are ever increasing numbers of non-traditional CNS targets currently being evaluated in the

clinic, many of which are characterized by larger and more polar ligands, such as proteases, kinases, and phosphodiesterases.^{144,145} It will be interesting to see how the median values of CNS drug properties change as these new approaches begin delivering drugs to the market.

Regardless, lipophilicity is likely to continue to be seen as the most critical physicochemical parameter and a robust predictor of clinical success across all therapeutic areas.⁹⁴ The essentially unchanging overall lipophilicity distribution in oral drugs over the past 40 years reflects the importance of balancing the impact of this property on the potency, pharmacokinetic, and safety profiles.⁸⁷ It is well-documented that increased lipophilicity is often accompanied not only by increased potency but also increased probability of reduced solubility and plasma free fraction as well as increased metabolic and toxicity liabilities.⁹⁴ For example, an analysis of the physicochemical properties and *in vivo* safety data relationships for 245 preclinical compounds at Pfizer showed a significantly higher risk of safety events for basic nitrogen containing compounds with $PS < 75 \text{ \AA}^2$ and $cLogP > 3$.¹⁴⁶ The inferred high-risk property profile significantly overlaps with the CNS drug property space, as described above, which further emphasizes the challenges associated with CNS drug discovery. With judicious selection of lead compounds and controlling lipophilicity during optimization by an effective use of efficiency parameters (LE, LLE, and LELP), medicinal chemists have an opportunity and responsibility to improve success rates in the clinic.⁹⁴

In contrast to lipophilicity, molecular descriptors related to hydrogen bonding are often found to be the dominant parameters impacting unbound drug brain concentrations. This is most likely a consequence of an additive combination of the two detrimental effects generally associated with hydrogen bonding, namely, poor passive permeability and increased risk of interactions with efflux transporters. An analysis of how oral drug properties have changed over time showed that the mean value of HBD count is constant, similar to $cLogP$ and PSA, suggesting that HBD is one of the most critical physicochemical properties, i.e., more important than HBA count.⁸⁷ Indeed, reducing the HBD count is one of the most frequently reported strategies that was successfully used in the optimization of brain exposure. An alternative strategy, which may be particularly attractive when HBDs are required for target activity, is the introduction of a suitably positioned HBA group to form an intramolecular H-bond. When increasing the PSA is undesirable, one could consider the incorporation of a halogen atom instead of HBA. Although considerably weaker than classical $O\cdots H$ and $N\cdots H$ H-bonds, improved property profiles have been reported in molecules that contain an intramolecular halogen bond.¹⁰⁷

Another important molecular property to consider in CNS drug discovery is aqueous solubility, which is at least in part a composite reflection of the physicochemical properties discussed earlier, as well as some of the more recently introduced structural descriptors such as carbon sp^3 fraction ($F_{sp^3} = \text{number of } sp^3\text{-hybridized carbons/total carbon count}$)¹⁴⁷ and aromatic ring count.¹⁴⁸ Alelyunas and colleagues at AstraZeneca reported that only 7 out of 98 marketed CNS drugs displayed measured solubility $< 10 \mu\text{M}$ in pH 7.4 buffer.¹⁴⁹ Interestingly, most of them were associated with significant safety issues for which they were either withdrawn or given a black box warning. The great majority of the CNS drugs in this set proved to be highly soluble compounds, with 85% displaying solubility $> 100 \mu\text{M}$.

The authors indicated that one could relate poor solubility with higher safety risks on the basis of its strong correlation with increased lipophilicity. It was suggested that compounds having solubility $< 1 \mu\text{M}$ are unlikely to become CNS drugs, while advancing compounds with solubility $< 10 \mu\text{M}$ would still bear high developability risks. The authors also pointed out a high risk of being outperformed by a competitor when advancing a poorly soluble compound. Improving solubility is one of the common objectives for fast follow-up programs. It is, therefore, tempting to consider aqueous solubility as one of the potential predictors of clinical success.

The majority of drugs bind to their targets by forming reversible noncovalent interactions, e.g., hydrogen bonds and hydrophobic interactions. For such agents, PK/PD relationships are usually well-understood in terms of equilibrium binding affinities (K_d) for their primary target relative to steady-state free plasma concentrations. However, in recent years, there has been a renewed and growing interest in the design of covalently bound inhibitors,¹⁵⁰ even for targets outside oncology indications that are historically associated with this approach, including CNS-related indications such as schizophrenia¹⁵¹ and pain.¹⁵² Several covalent irreversible inhibitors for CNS disorders have already been available on the market for many years (e.g., vigabatrin, selegiline, disulfiram), suggesting that this can be a safe and effective CNS drug discovery approach. Potential advantages of covalent inhibition include high potency and ligand efficiency, especially for less-druggable targets, which may translate to reduced dose and the associated body burden of the parent drug and its metabolites.¹⁵⁰ Due to nonequilibrium binding kinetics, covalent inhibitors of protein targets that regenerate slowly tend to display much longer pharmacodynamic half-lives than their pharmacokinetic half-lives.¹⁵³ For irreversible binders, free drug concentrations at the target coverage levels are generally needed only until the covalent interaction takes place, which often occurs relatively quickly (30 min to 1 h).¹⁵⁴ Consequently, this approach deemphasizes the need for compounds with long half-lives and high, prolonged systemic drug loads.¹⁵⁰ However, this potentially attractive aspect of the covalent binding approach may not be fully realized in CNS drug discovery for compounds with poor BBB penetration (e.g., $K_{puu} < 1$) that may require prolonged and high systemic exposure in order to achieve optimal target coverage in the brain. Hence, to minimize the risk of nonspecific irreversible tissue binding when pursuing covalent binders for CNS targets, while potentially compromising on drug half-life, one would be well-advised to focus, just as in reversible ligand programs, on designing compounds exhibiting physicochemical parameters conducive to good brain penetration properties, e.g., high P_{app} and no active efflux.

Many covalent inhibitors display high protein binding,¹⁵⁴ which, as discussed earlier,^{30,49} is not a liability per se, especially if most of the binding is reversible. The above-mentioned advantages of covalent irreversible inhibitors are critically balanced with the risk of idiosyncratic toxicity or immune-mediated hypersensitivity that may arise from nonspecific covalent binding.^{153,154} In this context, it is important to focus such drug discovery efforts on covalent binders with high specificity for the desired target(s) and with minimum off target nonspecific covalent tissue binding. To achieve this, one may focus on designing molecules with high reversible binding affinities, and containing chemically less reactive groups (warheads) in which covalent binding is a secondary and final interaction with the desired target, that occurs only when the

warhead is in a close proximity to the nucleophilic residue in the binding site. To potentially minimize the risks associated with irreversible binders, one may consider alternative approaches such as covalent reversible inhibition with slow K_{off} (e.g., rivastigmine) or arguably a more challenging prodrug approach (e.g., selegiline).^{150,151,155} In any case, a good aspirational goal for all drug discovery efforts has been provided by an observation that idiosyncratic toxicity is very rare among drugs administered at doses below 10 mg, regardless of the mode of action.^{156,157}

It is estimated that 98% of systemically administered small molecules, as well as nearly all biological therapeutics, i.e., recombinant proteins or gene-based medicines, are unable to cross the BBB.¹⁸ Enabling brain exposure for at least some of these molecules is the ultimate goal of the brain delivery systems.³⁴ Great progress has been made in recent years, particularly with some of the shuttle-mediated approaches that have proved to be successful in improving the CNS exposure of some of the small molecules synonymous with poor brain permeability, such as taxol.¹⁵⁸ However, further developments are needed for this approach to become a more robust mainstream technology with a general applicability. Until then, fine-tuning physicochemical properties for optimal brain exposure will remain a staple of CNS drug discovery.

■ ASSOCIATED CONTENT

Supporting Information

Calculated physicochemical properties and CNS MPO scores for a diverse set of compounds with experimentally obtained $C_{\text{u,b}}$ values (Figure 4). This material is available free of charge via the Internet at <http://pubs.acs.org>.

■ AUTHOR INFORMATION

Corresponding Author

*Phone: +1 (317) 277-3179; E-mail: rankovic_zoran@lilly.com, zoran.mailbox@gmail.com.

Notes

The author declares no competing financial interest.

Biography

Zoran Rankovic is a Research Fellow at Eli Lilly Headquarters, Indianapolis, Indiana, US. Before joining Eli Lilly in 2011, he was a medicinal chemistry director at Merck, Schering-Plough, and Organon UK. He started his industrial career at Organon in 1995, the same year he earned his Ph.D. in organic chemistry from the University of Leeds (UK), under the guidance of Professor Ronald Grigg. During his career, Zoran has been fortunate to be able to contribute to and lead teams that delivered multiple clinical candidates for a range of CNS disorders, including neurodegenerative, psychiatric, and pain indications. He is an author and coinventor on over 70 patents, scientific publications, and book chapters and an editor of two books on drug discovery topics.

■ ACKNOWLEDGMENTS

The author thanks Jibo Wang for constructing the MPO algorithm and Jeffrey J. Alberts and Mark G. Bures for helpful discussions and critical evaluations of the manuscript.

■ ABBREVIATIONS

P-gp, P-glycoprotein; CNS, central nervous system; ATP, adenosine-5'-triphosphate; SLC, solute carrier class; ABC, ATP-binding cassette; MRP, multidrug-resistance protein; BCRP, breast cancer resistance protein; BBB, blood-brain

barrier; BCSFB, blood-cerebrospinal fluid barrier; MDR, multidrug resistance; ER, efflux ratio; $A\beta$, amyloid β -peptide; MDCK, Madin-Darby canine kidney; LLC-PK, pig-kidney-derived epithelial; A-B, apical-to-basal; B-A, basal-to-apical; ER, efflux ratio; PAMPA, parallel artificial membrane permeability assay; ADMET, absorption, distribution, metabolism, excretion, and toxicity; logP, logarithm of the octanol/water partition coefficient; cLogP, calculated LogP; logD, logarithm of the octanol/water distribution coefficient at a given pH; cLogD, calculated LogD; MW, molecular weight; HBD, hydrogen-bond donors; HBA, hydrogen-bond acceptors; PSA, polar surface area; TPSA, topological polar surface area; RB, rotatable bonds; B/P, brain-to-plasma ratio; QSAR, quantitative structure-activity relationship; GPCR, G-protein coupled receptor; hERG, human ether- α -go related gene; ALK, anaplastic lymphoma kinase; WT, wild-type; KO, knockout; BACE, β -amyloid cleaving enzyme; p.o., per oral; s.c., subcutaneous; i.p., intraperitoneal; FDA, Food and Drug Administration; LE, ligand efficiency; MPO, multiparameter optimization; LLE, lipophilic ligand efficiency; LELP, ligand efficiency-dependent lipophilicity; LAT1, L-type amino acid transporter-1; RO, receptor occupancy

■ REFERENCES

- (1) Chandler, D. J. Something's got to give: psychiatric disease on the rise and novel drug development on the decline. *Drug Discovery Today* **2013**, *18*, 202–206.
- (2) *Forecasting Health Care Costs*; National Bureau of Economic Research: Cambridge, MA; <http://www.nber.org/aginghealth/2008no4/w14361.html>.
- (3) Barnholtz-Sloan, J. S.; Sloan, A. E.; Davis, F. G.; Vignea, F. D.; Lai, P.; Sawaya, R. E. Incidence proportions of brain metastases in patients diagnosed (1973 to 2001) in the metropolitan detroit cancer surveillance system. *J. Clin. Oncol.* **2004**, *22*, 2865–2872.
- (4) Siegel, R.; Ma, J.; Zou, Z.; Jemal, A. Cancer statistics. *Cancer J. Clin.* **2014**, *64*, 9–29 2014.
- (5) Nguyen, T. D.; DeAngelis, L. M. Brain metastases. *Neurol. Clin.* **2007**, *25*, 1173–1192.
- (6) Johnson, T. W.; Richardson, P. F.; Bailey, S.; Brooun, A.; Burke, B. J.; Collins, M. R.; Cui, J. J.; Deal, J. G.; Deng, Y.-L.; Dinh, D.; Engstrom, L. D.; He, M.; Hoffman, J.; Hoffman, R. L.; Huang, Q.; Kania, R. S.; Kath, J. C.; Lam, H.; Lam, J. L.; Le, P. T.; Lingardo, L.; Liu, W.; McTigue, M.; Palmer, C. L.; Sach, N. W.; Smeal, T.; Smith, G. L.; Stewart, A. E.; Timofeevski, S.; Zhu, H.; Zhu, J.; Zou, H. Y.; Edwards, M. P. Discovery of (10R)-7-Amino-12-fluoro-2,10,16-trimethyl-15-oxo-10,15,16,17-tetrahydro-2H-8,4-(metheno)pyrazolo-[4,3-h][2,5,11]-benzoxadiazacyclotetradecine-3-carbonitrile (PF-06463922), a macrocyclic inhibitor of anaplastic lymphoma kinase (ALK) and cros oncogene 1 (ROS1) with preclinical brain exposure and broad-spectrum potency against ALK-resistant mutations. *J. Med. Chem.* **2014**, *57*, 4720–4744.
- (7) Pardridge, W. M. The blood-brain barrier: bottleneck in brain drug development. *NeuroRx* **2005**, *2*, 3–14.
- (8) Shen, D. D.; Artru, A. A.; Adkison, K. K. Principles and applicability of CSF sampling for the assessment of CNS drug delivery and pharmacodynamics. *Adv. Drug Delivery Rev.* **2004**, *56*, 1825–1827.
- (9) Martin, I. Prediction of blood-brain barrier penetration: are we missing the point? *Drug Discovery Today* **2004**, *9*, 161–162.
- (10) Giacomini, K. M.; Huang, S.-M.; Tweedie, D. J.; Benet, L. Z.; Brouwer, K. L. R.; Chu, X.; Dahlin, A.; Evers, R.; Fischer, V.; Hillgren, K. M.; Hoffmaster, K. A.; Ishikawa, T.; Keppler, D.; Kim, R. B.; Lee, C. A.; Niemi, M.; Polli, J. W.; Sugiyama, Y.; Swaan, P. W.; Ware, J. A.; Wright, S. H.; Yee, S. W.; Zamek-Gliszczynski, M. J.; Zhang, L. Membrane transporters in drug development. *Nat. Rev. Drug Discovery* **2010**, *9*, 215–236.

- (11) Abbott, N. J.; Rönnebeck, L.; Hansson, L. Astrocyte–endothelial interactions at the blood–brain barrier. *Nat. Rev. Neurosci.* **2006**, *7*, 41–53.
- (12) Di, L.; Artursson, P.; Avdeef, A.; Ecker, G. F.; Faller, B.; Fischer, H.; Houston, J. B.; Kansy, M.; Kerns, E. H.; Kramer, S. D.; Lennernas, H.; Sugano, K. Evidence-based approach to assess passive diffusion and carrier-mediated drug transport. *Drug Discovery Today* **2012**, *17*, 905–912.
- (13) Rankovic, Z. Designing CNS drugs for optimal brain exposure. In *Blood–Brain Barrier in Drug Discovery: Optimizing Brain Exposure of CNS Drugs and Minimizing Brain Side Effects*, 1st ed.; Di, L., Kerns, E. H., Eds.; Wiley: New York, 2015.
- (14) Rankovic, Z.; Bingham, M. Medicinal chemistry challenges in CNS drug discovery. In *Drug Discovery for Psychiatric Disorders*, 1st ed.; Rankovic, Z., Bingham, M., Nestler, E., Hargreaves, R., Eds.; Royal Society of Chemistry: London, 2013; pp 465–509.
- (15) Hitchcock, S. A.; Pennington, L. D. Structure–brain exposure relationships. *J. Med. Chem.* **2006**, *49*, 7559–7583.
- (16) Malakoutikhah, M.; Teixid, M.; Giral, E. Shuttle-mediated drug delivery to the brain. *Angew. Chem., Int. Ed.* **2011**, *50*, 7998–8014.
- (17) Liu, X.; Chen, C. Strategies to optimize brain penetration in drug discovery. *Curr. Opin. Drug Discovery Dev.* **2005**, *8*, 505–512.
- (18) Liu, X.; Smith, B. J.; Chen, C.; Callegari, E.; Becker, S. L.; Chen, X.; Cianfrogna, J.; Doran, A. C.; Doran, S. D.; Gibbs, J. P.; Hosea, N.; Liu, J.; Nelson, F.; Szewc, M. A.; Deussen, J. V. Use of a physiologically based pharmacokinetic model to study the time to reach brain equilibrium: an experimental analysis of the role of blood–brain barrier permeability, plasma protein binding, and brain tissue binding. *J. Pharmacol. Exp. Ther.* **2005**, *313*, 1254–1262.
- (19) Pardridge, W. M. Blood–brain barrier delivery. *Drug Discovery Today* **2007**, *12*, 54–61.
- (20) Cecchelli, R.; Berzewski, V.; Lundquist, S.; Culot, M.; Renftel, M.; Dehouck, M.-P.; Fenart, L. Modelling of the blood–brain barrier in drug discovery and development. *Nat. Rev. Drug Discovery* **2007**, *6*, 50–661.
- (21) Maurer, T. S.; Debartolo, D. B.; Tess, D. A.; Scott, D. O. Relationship between exposure and nonspecific binding of thirty-three central nervous system drugs in mice. *Drug Metab. Dispos.* **2005**, *33*, 175–181.
- (22) Markus, P.; Vernaleken, I.; Roesch, F. Positron emission tomography in CNS drug discovery and drug monitoring. *J. Med. Chem.* **2014**, *57*, 9232–9258.
- (23) Di, L.; Rong, H.; Feng, B. Demystifying brain penetration in central nervous system drug discovery. *J. Med. Chem.* **2013**, *56*, 2–12.
- (24) Wu, D.; Kang, Y.-S.; Bickel, U.; Pardridge, W. M. Blood–brain barrier permeability to morphine-6-glucuronide is markedly reduced compared with morphine. *Drug Metab. Dispos.* **1997**, *26*, 768–771.
- (25) Frolich, N.; Dees, C.; Paetz, C.; Ren, X.; Lohse, M. J.; Nikolaev, V. O.; Zenk, M. H. Distinct pharmacological properties of morphine metabolites at Gi-protein and β -arrestin signaling pathways activated by the human μ -opioid receptor. *Biochem. Pharmacol.* **2011**, *81*, 1248–1254.
- (26) Paul, D.; Standiffer, K. M.; Inturrisi, C. E.; Pasternak, G. W. Pharmacological characterization of morphine 6-b-glucuronidase, a very potent morphine metabolite. *J. Pharmacol. Exp. Ther.* **1998**, *251*, 477–483.
- (27) Reichel, A. Addressing central nervous system (CNS) penetration in drug discovery: Basics and implications of the evolving new concept. *Chem. Biodivers.* **2009**, *6*, 2030–2049.
- (28) Stain-Textier, F.; Boschi, G.; Sandouk, P.; Scherrmann, J. M. Elevated concentrations of morphine 6-beta-d-glucuronide in brain extracellular fluid despite low blood–brain barrier permeability. *Br. J. Pharmacol.* **1999**, *128*, 917–924.
- (29) Gupta, A.; Hammarlund-Udenaes, M.; Chatelain, P.; Massingham, R.; Jonsson, E. N. Stereoselective pharmacokinetics of cetirizine in the guinea pig: role of protein binding. *Biopharm. Drug Dispos.* **2006**, *27*, 291–297.
- (30) Smith, D. A.; Di, L.; Kerns, E. H. The effect of plasma protein binding on in vivo efficacy: misconceptions in drug discovery. *Nat. Rev. Drug Discovery* **2010**, *9*, 929–939.
- (31) Polli, J. W.; Baughman, T. M.; Humphreys, J. E.; Jordan, K.H.; Mote, A. L.; Salisbury, J. A.; Tippin, T. K.; Serabjit-Singh, C. J. P-glycoprotein influences the brain concentrations of cetirizine (Zyrtec), a second-generation non-sedating antihistamine. *J. Pharm. Sci.* **2003**, *92*, 2082–2089.
- (32) Simon, F. E. R.; Simons, K. J. H1 antihistamines: current status and future directions. *World Allergy Organ. J.* **2008**, *1*, 145–155.
- (33) Sadiq, M. W.; Borgs, A.; Okura, T.; Shimomura, K.; Kato, S.; Deguchi, Y.; Jansson, B.; Bjoerkman, S.; Terasaki, T.; Hammarlund-udenaes, M. Diphenhydramine active uptake at the blood–brain barrier and its interaction with oxycodone *in vitro* and *in vivo*. *J. Pharm. Sci.* **2011**, *100*, 3912–3923.
- (34) Kageyama, T.; Nakamura, M.; Matsuo, A.; Yamasaki, Y.; Takakura, Y.; Hashida, M.; Kanai, Y.; Naito, M.; Tsuruo, T.; Minato, N.; Shimohama, S. The 4F2hc/LAT1 complex transports L-DOPA across the blood–brain barrier. *Brain Res.* **2000**, *879*, 115–121.
- (35) Doran, A.; Obach, R. S.; Smith, B. J.; Hosea, N. A.; Becker, S.; Callegari, E.; Chen, C.; Chen, X.; Choo, E.; Cianfrogna, J.; Cox, L. M.; Gibbs, J. P.; Gibbs, M. A.; Hatch, H.; Hop, C. E.; Kasman, I. N.; LaPerle, J.; Liu, J.; Liu, X.; Logman, M.; Maclin, D.; Nedza, F. M.; Nelson, F.; Olson, E.; Rahematpura, S.; Raunig, D.; Rogers, S.; Schmidt, K.; Spracklin, D. K.; Szewc, M.; Troutman, M.; Tseng, E.; Tu, M.; Van Deusen, J. W.; Venkatakrishnan, K.; Walens, G.; Wang, E. Q.; Wong, D.; Yasgar, A. S.; Zhang, C. The impact of P-glycoprotein on the disposition of drugs targeted for indications of the central nervous system: evaluation using the MDRIA/1B knockout mouse model. *Drug Metab. Dispos.* **2005**, *33*, 165–174.
- (36) Hammarlund-Udenaes, M.; Friden, S.; Synnen, M. S.; Gupta, A. On the rate and extent of drug delivery to the brain. *Pharm. Res.* **2008**, *25*, 1737–1750.
- (37) Wang, X.; Ratnaraj, N.; Patsalos, P. N. The pharmacokinetic inter-relationship of tiagabine in blood, cerebrospinal fluid and brain extracellular fluid (frontal cortex and hippocampus). *Seizure* **2004**, *13*, 574–581.
- (38) Friden, M.; Winiwarter, S.; Jerndal, G.; Bengtsson, O.; Wan, H.; Bredberg, U.; Hammarlund-Udenaes, M.; Antonsson, M. Structure–brain exposure relationships in rat and human using a novel data set of unbound drug concentrations in brain interstitial and cerebrospinal fluids. *J. Med. Chem.* **2009**, *52*, 6233.
- (39) Kodaira, H.; Kusuhara, H.; Fujita, T.; Ushiki, J.; Fuse, E.; Sugiyama, Y. Quantitative evaluation of the impact of active efflux by P-glycoprotein and breast cancer resistance protein at the blood–brain barrier on the predictability of the unbound concentrations of drugs in the brain using cerebrospinal fluid concentration as a surrogate. *J. Pharmacol. Exp. Ther.* **2011**, *339*, 935–944.
- (40) De Lange, E. C. M. Utility of CSF in translational neuroscience. *J. Pharmacokin. Pharmacodyn.* **2013**, *40*, 315–326.
- (41) Westerhout, J.; Danhof, M.; De Lange, E. C. M. Preclinical prediction of human brain target site concentrations: Considerations and extrapolating to the clinical setting. *J. Pharm. Sci.* **2011**, *100*, 3577–3593.
- (42) Wan, H.; Rehgren, M.; Giordanetto, F.; Bergström, F.; Tunek, A. High-throughput screening of drug–brain tissue binding and *in silico* prediction for assessment of central nervous system drug delivery. *J. Med. Chem.* **2007**, *50*, 4606–4615.
- (43) Friden, M.; Gupta, A.; Antonsson, M.; Bredberg, U.; Hammarlund-Udenaes, M. *In vitro* methods for estimating unbound drug concentrations in the brain interstitial and intracellular fluids. *Drug Metab. Dispos.* **2007**, *35*, 1711–1719.
- (44) Liu, X.; Natta, K.; van Yeo, H.; Vilenski, O.; Weller, P.; Worboys, P.; Monshouwer, M. Unbound drug concentration in brain homogenate and cerebral spinal fluid at steady state as a surrogate for unbound concentration in brain interstitial fluid. *Drug Metab. Dispos.* **2009**, *37*, 787–793.

- (45) Debruyne, D. Clinical pharmacokinetics of fluconazole in superficial and systemic mycoses. *Clin. Pharmacokinet.* **1997**, *33*, 52–77.
- (46) Summerfield, S. G.; Lucas, A. J.; Porter, R. A.; Jeffrey, P.; Gunn, R. N.; Read, K. R.; Stevens, A. J.; Metcalf, A. C.; Osuna, M. C.; Kilford, P. J.; Passchier, J.; Ruffo, A. D. Toward an improved prediction of human *in vivo* brain penetration. *Xenobiotica* **2008**, *38*, 1518–1535.
- (47) Di, L.; Umland, J. P.; Chang, G.; Huang, Y.; Lin, Z.; Scott, D. O.; Troutman, M. D.; Liston, T. E. Species independence in brain tissue binding using brain homogenates. *Drug Metab. Dispos.* **2011**, *39*, 1270–1277.
- (48) Jeffrey, P.; Summerfield, S. G. Challenges for blood–brain barrier (BBB) screening. *Xenobiotica* **2007**, *37*, 1135–1151.
- (49) Liu, X.; Wright, M.; Hop, C. E. C. A. Rational use of plasma protein and tissue binding data in drug design. *J. Med. Chem.* **2014**, *57*, 8238–8248.
- (50) Garberg, P.; Ball, M.; Borg, N.; Cecchelli, R.; Fenart, L.; Hurst, R. D.; Lindmark, T.; Mabondzo, A.; Nilsson, J. E.; Raub, T. J.; Stanimirovic, D.; Terasaki, T.; Oeberg, J. O.; Oesterberg, T. *In-vitro* models for the blood brain barrier. *Toxicol. In Vitro* **2005**, *19*, 299–334.
- (51) Kansy, M.; Senner, F.; Gubernator, K. Physicochemical high throughput screening: parallel artificial membrane permeation assay in the description of passive absorption processes. *J. Med. Chem.* **1998**, *41*, 1007–1010.
- (52) Veber, D. F.; Johnson, S. R.; Chen, H.-Y.; Smith, B. R.; Ward, K. W.; Kopple, K. D. Molecular properties that influence the oral bioavailability of drug candidates. *J. Med. Chem.* **2002**, *45*, 2615–2623.
- (53) Giacomini, K. M.; Huang, S.-M.; Tweedie, D. J.; Benet, L. Z.; Brouwer, K. L. R.; Chu, X.; Dahlin, A.; Evers, R.; Fischer, V.; Hillgren, K. M.; Hoffmaster, K. A.; Ishikawa, T.; Keppler, D.; Kim, R. B.; Lee, C. A.; Niemi, M.; Polli, J. W.; Sugiyama, Y.; Swaan, P. W.; Ware, J. A.; Wright, S. H.; Yee, S. W.; Zamek-Gliszczynski, M. J.; Zhang, L. Membrane transporters in drug development. *Nat. Rev. Drug Discovery* **2010**, *9*, 215–236.
- (54) Hitchcock, S. A. Structural modifications that alter the P-glycoprotein efflux properties of compounds. *J. Med. Chem.* **2012**, *55*, 4877–4895.
- (55) Sharom, F. J. The P-glycoprotein efflux pump: how does it transport drugs? *J. Membr. Biol.* **1997**, *160*, 161–175.
- (56) Cordon-Cardo, C.; O'Brien, J. P.; Casals, D.; Rittman-Grauer, L.; Biedler, J. L.; Melamed, M. R.; Bertino, J. R. Multidrug-resistance gene (P-glycoprotein) is expressed by endothelial cells at blood-brain barrier sites. *Proc. Natl. Acad. Sci. U.S.A.* **1989**, *86*, 695–698.
- (57) Doan, M. K. M.; Humphreys, J. E.; Webster, L. O.; Wring, S. A.; Shampine, L. J.; Serabjit-Singh, C. J.; Adkinson, K. K.; Polli, J. W. Passive permeability and P-glycoprotein-mediated efflux differentiate central nervous system (CNS) and non-CNS marketed drugs. *J. Pharmacol. Exp. Ther.* **2002**, *303*, 1029–1037.
- (58) Demeule, M.; Regina, A.; Jodoin, J.; Laplante, A.; Dagenais, C.; Berthelet, F.; Moghrabi, A.; Beliveau, R. Drug transport to the brain: Key roles for the efflux pump P-glycoprotein in the blood–brain barrier. *Vasc. Pharmacol.* **2002**, *38*, 339–348.
- (59) Feng, B.; Mills, J. B.; Davidson, R. E.; Mireles, R. J.; Janiszewski, J. S.; Troutman, M. D.; de Morais, S. M. *In vitro* P-glycoprotein assays to predict the *in vivo* interactions of P-glycoprotein with drugs in the central nervous system. *Drug Metab. Dispos.* **2008**, *36*, 268–275.
- (60) Hsiao, P.; Sasongko, L.; Link, J. M.; Mankoff, D. A.; Muzi, M.; Collier, A. C.; Unadkat, J. D. Verapamil P-glycoprotein transport across the rat blood–brain barrier: cyclosporine, a concentration inhibition analysis, and comparison with human data. *J. Pharmacol. Exp. Ther.* **2006**, *317*, 704–710.
- (61) Aller, S. G.; Yu, J.; Ward, A.; Weng, Y.; Chittaboina, S.; Zhuo, R.; Harrell, P. M.; Trinh, Y. T.; Zhang, Q.; Urbatsch, I. L.; Chang, G. Structure of P-glycoprotein reveals a molecular basis for poly-specific drug binding. *Science* **2009**, *323*, 1718–1722.
- (62) Desai, P. V.; Raub, T. J.; Blanco, M.-J. How hydrogen bonds impact P-glycoprotein transport and permeability. *Bioorg. Med. Chem. Lett.* **2012**, *22*, 6540–6548.
- (63) Raub, T. J.; Lutzke, B. S.; Andrus, P. K.; Sawada, G. A.; Staton, B. A. Early preclinical evaluation of brain exposure in support of hit identification and lead optimization. In *Optimizing the 'Drug-Like' Properties of Leads in Drug Discovery*, 1st ed.; Borchardt, R. T., Kerns, E. H., Hageman, M. J., Thakker, D. R., Stevens, J. L., Eds.; Springer: New York, 2006; pp 355–410.
- (64) Doyle, L. A.; Yang, W.; Abruzzo, L. V.; Kroghmann, T.; Gao, Y.; Rishi, A. K.; Ross, D. D. A multidrug resistance transporter from human MCF-7 breast cancer cells. *Proc. Natl. Acad. Sci. U.S.A.* **1998**, *95*, 15665–15670.
- (65) Eisenblatter, T.; Galla, H. J. A new multidrug resistance protein at the blood-brain barrier. *Biochem. Biophys. Res. Commun.* **2002**, *293*, 1273–1278.
- (66) Chen, Y.; Agarwal, S.; Shaik, N. M.; Chen, C.; Yang, Z.; Elmquist, W. F. P-glycoprotein and breast cancer resistance protein influence brain distribution of dasatinib. *J. Pharmacol. Exp. Ther.* **2009**, *330*, 956–63.
- (67) Tang, S. C.; Lagas, J. C.; Lankheet, N. A. G.; Poller, B.; Hillebrand, M. J.; Rosing, H.; Beijnen, J. H.; Schinkel, A. H. Brain accumulation of sunitinib is restricted by P-glycoprotein (ABCB1) and breast cancer resistance protein (ABCG2) and can be enhanced by oral elacridar and sunitinib coadministration. *Int. J. Cancer* **2012**, *130*, 223–233.
- (68) Zhao, R.; Raub, T. J.; Sawada, G. A.; Kasper, S. C.; Bacon, J. A.; Bridges, A. S.; Pollack, G. M. Breast cancer resistance protein interacts with various compounds *in vitro*, but plays a minor role in substrate efflux at the blood–brain barrier. *Drug Metab. Dispos.* **2009**, *37*, 1251–1258.
- (69) Giri, N.; Shaik, N.; Pan, G.; Terasaki, T.; Mukai, C.; Kitagaki, S.; Miyakoshi, N.; Elmquist, W. F. Investigation of the role of breast cancer resistance protein (Bcrp/Abcg2) on pharmacokinetics and central nervous system penetration of abacavir and zidovudine in the mouse. *Drug Metab. Dispos.* **2008**, *36*, 1476–1484.
- (70) Ball, K.; Bouzom, F.; Scherrmann, J.-M.; Walther, B.; Declèves, X. Physiologically based pharmacokinetic modelling of drug penetration across the blood–brain barrier—Towards a mechanistic IVIVE-based approach. *AAPS J.* **2013**, *15*, 913–932.
- (71) Ball, K.; Bouzom, F.; Scherrmann, J.-M.; Walther, B.; Declèves, X. Development of a physiologically based pharmacokinetic model for the rat central nervous system and determination of an *in vitro*–*in vivo* scaling methodology for the blood–brain barrier permeability of two transporter substrates, morphine and oxycodone. *J. Pharm. Sci.* **2012**, *101*, 4277–4292.
- (72) Eyal, S.; Hsiao, P.; Unadkat, J. D. Drug interactions at the blood–brain barrier: fact or fantasy? *Pharmacol. Ther.* **2009**, *123*, 80–104.
- (73) Kalvass, J. C.; Polli, J. W.; Bourdet, D. L.; Feng, B.; Huang, S.-M.; Liu, X.; Smith, Q. R.; Zhang, L. K.; Zamek-Gliszczynski, M. J. Why clinical modulation of efflux transport at the human blood–brain barrier is unlikely: the ITC evidence-based position. *Clin. Pharmacol. Ther.* **2013**, *94*, 80–94.
- (74) Schinkel, A. H.; Mayer, U.; Wagenaar, E.; Mol, C. A. A. M.; van Deemter, L.; Smit, J. J. M.; van der Valk, M. A.; Voordouw, A. C.; Spits, H.; van Tellingen, O.; Zijlmans, J. M.; Fibbe, W. E.; Borst, P. Normal viability and altered pharmacokinetics in mice lacking mdr1-type (drug-transporting) P-glycoproteins. *Proc. Natl. Acad. Sci. U.S.A.* **1997**, *94*, 4028–4033.
- (75) Cutler, L.; Howes, C.; Deeks, N. J.; Buck, T. L.; Jeffrey, P. Development of a P-glycoprotein knockout model in rodents to define species differences in its functional effect at the blood–brain barrier. *J. Pharm. Sci.* **2006**, *95*, 1944–1953.
- (76) Syvanen, S.; Lindhe, O.; Palner, M.; Kornum, B. R.; Rahman, O.; Langstrom, B.; Knudsen, G. M.; Hammarlund-Udenaes, M. Species differences in blood–brain barrier transport of three positron emission tomography radioligands with emphasis on P-glycoprotein transport. *Drug Metab. Dispos.* **2009**, *37*, 635–643.
- (77) Desai, P. V.; Sawada, G. A.; Watson, I. A.; Raub, T. J. Integration of *in silico* and *in vitro* tools for scaffold optimization during drug

discovery: predicting P-glycoprotein efflux. *Mol. Pharmaceutics* **2013**, *10*, 1249–1261.

(78) Didziapetris, R.; Japertas, P.; Avdeef, A.; Petrauskas, A. Classification analysis of P-glycoprotein substrate specificity. *J. Drug Targeting* **2003**, *11*, 391–406.

(79) Del Amo, E. M.; Urtti, A.; Yliperttula, M. Pharmacokinetic role of L-type amino acid transporters LAT1 and LAT2. *Eur. J. Pharm. Sci.* **2008**, *35*, 161–174.

(80) Lipinski, C. A.; Lombardo, F.; Dominy, B. W.; Feeney, P. J. Experimental and computational approaches to estimate solubility and permeability in drug discovery and development settings. *Adv. Drug Del. Rev.* **1997**, *23*, 3–26.

(81) Ghose, A. K.; Herbertz, T.; Hudkins, R. L.; Dorsey, B. D.; Mallamo, J. P. Knowledge-based, central nervous system (CNS) lead selection and lead optimization for CNS drug discovery. *ACS Chem. Neurosci.* **2012**, *3*, 50–68.

(82) Wager, T. T.; Chandrasekaran, R. Y.; Hou, X.; Troutman, M. D.; Verhoest, P. R.; Villalobos, A.; Will, Y. Defining desirable central nervous system drug space through the alignment of molecular properties, *in vitro* ADME, and safety attributes. *ACS Chem. Neurosci.* **2010**, *1*, 420–434.

(83) Wager, T. T.; Hou, X.; Verhoest, P. R.; Villalobos, A. Moving beyond rules: the development of a central nervous system multiparameter optimization (CNS MPO) approach to enable alignment of druglike properties. *ACS Chem. Neurosci.* **2010**, *1*, 435–439.

(84) Waring, M. J. Defining optimum lipophilicity and molecular weight ranges for drug candidates—molecular weight dependent lower logD limits based on permeability. *Bioorg. Med. Chem. Lett.* **2009**, *19*, 2844–2851.

(85) Gleeson, M. P. Generation of a set of simple, interpretable ADMET rules of thumb. *J. Med. Chem.* **2008**, *51*, 817–834.

(86) Pajouhesh, H.; Lenz, G. R. Medicinal chemical properties of successful central nervous system drugs. *NeuroRx* **2005**, *2*, 541–553.

(87) Leeson, P. D.; Davis, A. M. Time-related differences in the physical property profiles of oral drugs. *J. Med. Chem.* **2004**, *47*, 6338–6348.

(88) Norinder, U.; Haerberlein, M. Computational approaches to the prediction of the blood–brain distribution. *Adv. Drug Deliv. Rev.* **2002**, *54*, 291–313.

(89) Kelder, J.; Grootenhuis, P. D. J.; Bayada, D. M.; Delbressine, L. P. C.; Ploemen, J.-P. Polar molecular surface as a dominating determinant for oral absorption and brain penetration of drugs. *Pharm. Res.* **1999**, *16*, 1514–1519.

(90) Van de Waterbeemd, H.; Camenisch, G.; Folkers, G.; Chretien, J. R.; Raevsky, O. A. Estimation of blood–brain barrier crossing of drugs using molecular size and shape, and H-bonding descriptors. *J. Drug Targeting* **1998**, *6*, 151–165.

(91) Van de Waterbeemd, H.; Kansy, M. Hydrogen-bonding capacity and brain penetration. *Chimia* **1992**, *46*, 299–303.

(92) Young, R. C.; Mitchell, R. C.; Brown, T. H.; Ganellin, C. R.; Griffiths, R.; Jones, M.; Rana, K. K.; Saunders, D.; Smith, I. R.; Sore, N. E.; Wilks, T. J. Development of a new physicochemical model for brain penetration and its application to the design of centrally acting H₂ receptor histamine antagonists. *J. Med. Chem.* **1988**, *31*, 656–671.

(93) Hansch, C.; Steward, A. R.; Anderson, S. M.; Bentley, D. L. Parabolic dependence of drug action upon lipophilic character as revealed by a study of hypnotics. *J. Med. Chem.* **1968**, *1*, 1–11.

(94) Leeson, P. D.; Springthorpe, B. The influence of drug-like concepts on decision-making in medicinal chemistry. *Nat. Rev. Drug Discovery* **2007**, *6*, 881–890.

(95) Leo, A.; Hansch, C.; Elkins, D. Partition coefficients and their uses. *Chem. Rev.* **1971**, *71*, 525–616.

(96) Johnson, D. J.; Forbes, I. T.; Watson, S. P.; Garzya, V.; Stevenson, G. I.; Walker, G. R.; Mudhar, H. S.; Flynn, S. J.; Wyman, P. A.; Smith, P. W.; Murkitt, G. S.; Lucas, A. J.; Mookherjee, C. R.; Watson, J. M.; Gartlon, J. E.; Bradford, A. M.; Brown, F. The discovery of a series of N-substituted 3-(4-piperidinyl)-1,3-benzoxazolinones and

oxindoles as highly brain penetrant, selective muscarinic M1 agonists. *Bioorg. Med. Chem. Lett.* **2010**, *20*, 5434–5438.

(97) Smith, P. W.; Wyman, P. A.; Lovell, P.; Goodacre, C.; Serafinowska, H. T.; Vong, A.; Harrington, F.; Flynn, S.; Bradley, D. M.; Porter, R.; Coggon, S.; Murkitt, G.; Searle, K.; Thomas, D. R.; Watson, J. M.; Martin, W.; Wu, Z.; Dawson, L. A. New quinoline NK3 receptor antagonists with CNS activity. *Bioorg. Med. Chem. Lett.* **2009**, *19*, 837–840.

(98) Martin, Y. C. A bioavailability score. *J. Med. Chem.* **2005**, *48*, 3164–3170.

(99) Abraham, M. H. Scales of solute hydrogen-bonding: their construction and application to physicochemical and biochemical processes. *Chem. Soc. Rev.* **1993**, *22*, 73–83.

(100) Kuduk, S. D.; Di Marco, C. N.; Chang, R. K.; Wood, M. R.; Schirripa, K. M.; Kim, J. J.; Wai, J. M.; DiPardo, R. M.; Murphy, K. L.; Ransom, R. W.; Harrell, C. M.; Reiss, D. R.; Holahan, M. A.; Cook, J.; Hess, J. F.; Sain, N.; Urban, M. O.; Tang, C.; Prueksaranont, T.; Pettibone, D. J.; Bock, M. G. Development of orally bioavailable and CNS penetrant biphenylaminocyclopropane carboxamide bradykinin B1 receptor antagonists. *J. Med. Chem.* **2007**, *50*, 272–282.

(101) Hu, E.; Kunz, R. K.; Chen, N.; Rumfelt, S.; Siegmund, A.; Andrews, K.; Chmait, S.; Zhao, S.; Davis, C.; Chen, H.; Lester-Zeiner, D.; Ma, J.; Biorn, C.; Shi, J.; Porter, A.; Treanor, J.; Allen, J. R. Design, optimization, and biological evaluation of novel keto-benzimidazoles as potent and selective inhibitors of phosphodiesterase 10A (PDE10A). *J. Med. Chem.* **2013**, *56*, 8781–8792.

(102) Kuhn, B.; Mohr, P.; Stahl, M. Intramolecular hydrogen bonding in medicinal chemistry. *J. Med. Chem.* **2010**, *53*, 2601–2611.

(103) Rafi, S. B.; Hearn, B. R.; Vedantham, P.; Jacobson, M. P.; Renslo, A. R. Predicting and improving the membrane permeability of peptidic small molecules. *J. Med. Chem.* **2012**, *55*, 3163–3169.

(104) Ashwood, V. A.; Field, M. J.; Horwell, D. C.; Julien-Larose, C.; Lewthwaite, R. A.; McCleary, S.; Pritchard, M. C.; Raphy, J.; Singh, L. Utilization of an intramolecular hydrogen bond to increase the CNS penetration of an NK1 receptor antagonist. *J. Med. Chem.* **2001**, *44*, 2276–2285.

(105) Over, B.; McCarren, P.; Artursson, P.; Foley, M.; Giordanetto, F.; Grönberg, G.; Hilgendorf, C.; Lee, M. D.; Matsson, P.; Muncipinto, G.; Pellissier, M.; Perry, M. W. D.; Svensson, R.; Duvall, J. R.; Kihlberg, J. Impact of stereospecific intramolecular hydrogen bonding on cell permeability and physicochemical properties. *J. Med. Chem.* **2014**, *57*, 2746–2754.

(106) Hennig, L.; Ayala-Leon, K.; Angulo-Cornejo, J.; Richter, R.; Beyer, L. Fluorine hydrogen short contacts and hydrogen bonds in substituted benzamides. *J. Fluorine Chem.* **2009**, *130*, 453–460.

(107) Weiss, M. M.; Williamson, T.; Babu-Khan, S.; Bartberger, M. D.; Brown, J.; Chen, K.; Cheng, Y.; Citron, M.; Croghan, M. D.; Dineen, T. A.; Esmay, J.; Graceffa, R. F.; Harried, S. S.; Hickman, D.; Hitchcock, S. A.; Horne, D. B.; Huang, H.; Imbeah-Ampiah, R.; Judd, T.; Kaller, M. R.; Kreiman, C. R.; La, D. S.; Li, V.; Lopez, P.; Louie, S.; Monenschein, H.; Nguyen, T. T.; Pennington, L. D.; Rattan, C.; San Miguel, T.; Sickmier, E. A.; Wahl, R. C.; Wen, P. H.; Wood, S.; Xue, Q.; Yang, B. H.; Patel, V. F.; Zhong, W. Design and preparation of a potent series of hydroxyethylamine containing β -secretase inhibitors that demonstrate robust reduction of central β -amyloid. *J. Med. Chem.* **2012**, *55*, 9009–9024.

(108) Yuan, J.; Venkatraman, S.; Zheng, Y.; McKeever, B. M.; Dillard, L. W.; Singh, S. B. Structure-based design of β -site APP cleaving enzyme 1 (BACE1) inhibitors for the treatment of Alzheimer's disease. *J. Med. Chem.* **2013**, *56*, 4156–4180.

(109) Alex, A.; Millan, D. S.; Perez, M.; Wakenhut, F.; Whitlock, G. A. Intramolecular hydrogen bonding to improve membrane permeability and absorption in beyond rule of five chemical space. *Med. Chem. Commun.* **2011**, *2*, 669–674.

(110) Baxter, N. J.; Williamson, M. P. Temperature dependence of ¹H chemical shifts in proteins. *J. Biomol. NMR* **1997**, *9*, 359–369.

(111) Tardia, P.; Stefanachi, A.; Niso, M.; Stolfi, D. A.; Mangiatordi, G. F.; D'Alberga, D.; Nicolotti, O.; Lattanzi, G.; Carotti, A.; Leonetti, F.; Perrone, R.; Berardi, F.; Azzariti, A.; Colabufo, N. A.; Cellamare, S.

Trimethoxybenzamide-based P-glycoprotein modulators: an interesting case of lipophilicity tuning by intramolecular hydrogen bonding. *J. Med. Chem.* **2014**, *57*, 6403–6418.

(112) Shalaeva, M.; Caron, G.; Abramov, Y. A.; O'Connell, T. N.; Plummer, M. S.; Yalamanchi, G.; Farley, K. A.; Goetz, G. H.; Philippe, L.; Shapiro, M. J. Integrating intramolecular hydrogen bonding (IMHB) considerations in drug discovery using $\Delta\log P$ as a tool. *J. Med. Chem.* **2013**, *56*, 4870–4879.

(113) Goetz, H.; Farrell, W.; Shalaeva, M.; Sciabola, S.; Anderson, D.; Yan, J.; Philippe, L.; Shapiro, M. J. High throughput method for the indirect detection of intramolecular hydrogen bonding. *J. Med. Chem.* **2014**, *57*, 2920–2929.

(114) Ertl, P.; Rohde, B.; Selzer, P. Fast calculation of molecular polar surface area as a sum of fragment-based contributions and its application to the prediction of drug transport properties. *J. Med. Chem.* **2000**, *43*, 3714–3717.

(115) Palm, K.; Luthman, K.; Ungell, A. L.; Strandlund, G.; Artursson, P. Correlation of drug absorption with molecular surface properties. *J. Pharm. Sci.* **1996**, *85*, 32–39.

(116) Richmond, T. J. T. Solvent accessible surface area and excluded volume in proteins. *J. Mol. Biol.* **1984**, *178*, 63–89.

(117) Goldberg, F. W.; Dossetter, A. G.; Scott, J. S.; Robb, R.; Boyd, S.; Groombridge, S. D.; Kemmitt, P. D.; Sjogren, T.; Gutierrez, P. M.; De Schoolmeester, J.; Swales, J. G.; Turnbull, A. W.; Wild, M. J. Optimization of brain penetrant 11β -hydroxysteroid dehydrogenase type I inhibitors and *in vivo* testing in diet-induced obese mice. *J. Med. Chem.* **2014**, *57*, 970–986.

(118) Ward, S. E.; Harries, M.; Aldegheri, L.; Andreotti, D.; Ballantine, S.; Bax, B. D.; Harris, A. J.; Harker, A. J.; Lund, J.; Melarange, R.; Mingardi, A.; Mookherjee, C.; Mosley, J.; Neve, M.; Oliosi, B.; Profeta, R.; Smith, K. J.; Smith, P. W.; Spada, S.; Thewlis, K. M.; Yusaf, S. P. Discovery of *N*-[(2*S*)-5-(6-fluoro-3-pyridinyl)-2,3-dihydro-1*H*-inden-2-yl]-2-propanesulfonamide, a novel clinical AMPA receptor positive modulator. *J. Med. Chem.* **2010**, *53*, 5801–5812.

(119) McDonald, I. M.; Mate, R. A.; Zusi, F. C.; Huang, H.; Post-Munson, D. J.; Ferrante, M. A.; Gallagher, L.; Bertekap, R. L., Jr.; Knox, R. J.; Robertson, B. J.; Harden, D. G.; Morgan, D. G.; Lodge, N. J.; Dworetzky, S. I.; Olson, R. E.; Macor, J. E. Discovery of a novel series of quinolone $\alpha 7$ nicotinic acetylcholine receptor agonists. *Bioorg. Med. Chem. Lett.* **2013**, *23*, 1684–1688.

(120) Lerchner, A.; Machauer, R.; Betschart, C.; Veenstra, S.; Rueeger, H.; McCarthy, C.; Tintelnot-Blomley, M.; Jatou, A.-L.; Rabe, S.; Desrayaud, S.; Enz, A.; Staufienbiel, M.; Paganetti, P.; Rondeau, J.-M.; Neumann, U. Macrocyclic BACE-1 inhibitors acutely reduce $A\beta$ in brain after po application. *Bioorg. Med. Chem. Lett.* **2010**, *20*, 603–607.

(121) Rampe, D.; Wible, B.; Brown, A. M.; Dage, R. C. Effects of terfenadine and its metabolites on a delayed rectifier K1 channel cloned from human heart. *Mol. Pharmacol.* **1993**, *44*, 1240–1245.

(122) Doan, M. K. M.; Wring, S. A.; Shampine, L. J.; Jordan, K. H.; Bishop, J. P.; Kratz, J.; Yang, E.; Serabjit-Singh, C. J.; Adkison, K. K.; Polli, J. W. Steady-state brain concentrations of antihistamines in rats: interplay of membrane permeability, P-glycoprotein efflux and plasma protein binding. *Pharmacology* **2004**, *72*, 92–98.

(123) Zhao, R.; Kalvass, J. C.; Yanni, S. B.; Bridges, A. S.; Pollack, G. M. Fexofenadine brain exposure and the influence of blood-brain barrier P-glycoprotein after fexofenadine and terfenadine administration. *Drug Metab. Dispos.* **2009**, *37*, 529–535.

(124) Mihalic, J. T.; Fan, F.; Chen, X.; Chen, X.; Fu, Y.; Motani, A.; Liang, L.; Lindstrom, M.; Tang, L.; Chen, L.-L.; Jaen, J.; Dai, K.; Li, L. Discovery of a novel melanin concentrating hormone receptor 1 (MCHR1) antagonist with reduced hERG inhibition. *Bioorg. Med. Chem. Lett.* **2012**, *22*, 3781–3785.

(125) Hogberg, T.; Frimurer, T.; Sasmal, P. K. Melanin concentrating hormone receptor 1 (MCHR1) antagonists—still a viable approach for obesity treatment? *Bioorg. Med. Chem. Lett.* **2012**, *22*, 6039–6047.

(126) Jamieson, C.; Moir, E. M.; Rankovic, Z.; Wishart, G. Medicinal chemistry of hERG optimizations: highlights and hang-ups. *J. Med. Chem.* **2006**, *49*, 5029–5050.

(127) Gianotti, M.; Botta, M.; Brough, S.; Carletti, R.; Castiglioni, E.; Corti, C.; Dal-Cin, M.; Fratte, S. D.; Korajac, D.; Lovric, M.; Merlo, G.; Mesic, M.; Pavone, F.; Piccoli, L.; Rast, S.; Roscic, M.; Sava, A.; Smehil, M.; Stasi, L.; Togninelli, A.; Wigglesworth, M. J. Novel spirotricyclic zwitterionic dual H1/5-HT2A receptor antagonists for the treatment of sleep disorders. *J. Med. Chem.* **2010**, *53*, 7778–7795.

(128) McCoull, W.; Barton, P.; Brown, A. J. H.; Bowker, S. S.; Cameron, J.; Clarke, D. S.; Davies, R. D. M.; Dossetter, A. G.; Ertan, A.; Fenwick, M.; Green, C.; Holmes, J. L.; Martin, N.; Masters, D.; Moore, J. E.; Newcombe, N. J.; Newton, C.; Pointon, H.; Robb, G. R.; Sheldon, C.; Stokes, S.; Morgan, D. Identification, optimization, and pharmacology of acylurea GHS-R1a inverse agonists. *J. Med. Chem.* **2014**, *57*, 6128–6140.

(129) Costa, D. B.; Kobayashi, S.; Pandya, S. S.; Yeo, W. L.; Shen, Z.; Tan, W.; Wilner, K. D. CSF concentration of the anaplastic lymphoma kinase inhibitor crizotinib. *J. Clin. Oncol.* **2011**, *29*, 443–445.

(130) Marsault, E.; Peterson, M. L. Macrocycles are great cycles: applications, opportunities, and challenges of synthetic macrocycles in drug discovery. *J. Med. Chem.* **2011**, *54*, 1961–2004.

(131) Levin, V. A. Relationship of octanol/water partition coefficients to rat brain capillary permeability. *J. Med. Chem.* **1980**, *23*, 682–684.

(132) Hopkins, A. L.; Groom, C. R.; Alex, A. Ligand efficiency: a useful metric for lead selection. *Drug Discovery Today* **2004**, *9*, 430–431.

(133) Bergstrom, C. A. S.; Strafford, M.; Lazorova, L.; Avdeef, A.; Luthman, K.; Artursson, P. Absorption classification of oral drugs based on molecular surface properties. *J. Med. Chem.* **2003**, *46*, 558–570.

(134) Tantishaiyakul, V. Prediction of Caco-2 cell permeability using partial least square multivariate analysis. *Pharmazie* **2001**, *56*, 407–411.

(135) Egan, W. J.; Merz, K. M., Jr.; Baldwin, J. J. Prediction of drug absorption using multivariate statistics. *J. Med. Chem.* **2000**, *43*, 3867–3877.

(136) Keseru, G. M.; Makara, G. M. The influence of lead discovery strategies on the properties of drug candidates. *Nat. Rev. Drug Discovery* **2009**, *8*, 203–212.

(137) Tarcsay, A.; Nyiri, K.; Keseru, G. M. Impact of lipophilic efficiency on compound quality. *J. Med. Chem.* **2012**, *55*, 1252–1260.

(138) Nicolaou, C. A.; Brown, N. Multi-objective optimization methods in drug design. *Drug Discovery Today: Technol.* **2013**, *10*, 427–435.

(139) Shen, J.; Cheng, F.; Xu, Y.; Li, W.; Tang, Y. Estimation of ADME properties with substructure pattern recognition. *J. Chem. Inf. Model.* **2010**, *50*, 1034–1041.

(140) Chernet, E.; Martin, L. J.; Li, D.; Need, A. B.; Barth, V. N.; Rash, K. S.; Phebus, L. A. Use of LC/MS to assess brain tracer distribution in preclinical, *in vivo* receptor occupancy studies: dopamine D2, serotonin 2A and NK-1 receptors as examples. *Life Sci.* **2005**, *78*, 340–346.

(141) Need, A. B.; McKinzie, J. H.; Mitch, C. H.; Statnick, M. A.; Phebus, L. A. *In vivo* rat brain opioid receptor binding of LY255582 assessed with a novel method using LC/MS/MS and the administration of three tracers simultaneously. *Life Sci.* **2007**, *81*, 1389–1396.

(142) Hawkins, B. T.; Davis, T. P. The blood–brain barrier/neurovascular unit in health and disease. *Am. Soc. Pharmacol. Exp. Ther.* **2005**, *57*, 173–185.

(143) Seelbach, M. J.; Brooks, T. A.; Egleton, R. D.; Davis, T. P. Peripheral inflammatory hyperalgesia modulates morphine delivery to the brain: a role for P-glycoprotein. *J. Neurochem.* **2007**, *102*, 1677–1690.

(144) Vieth, M.; Siegel, M. G.; Higgs, R. E.; Watson, I. A.; Robertson, D. H.; Savin, K. A.; Durst, G. L.; Hipskind, P. A. Characteristic physical properties and structural fragments of marketed oral drugs. *J. Med. Chem.* **2004**, *47*, 224–232.

(145) Morphy, R. The influence of target family and functional activity on the physicochemical properties of pre-clinical compounds. *J. Med. Chem.* **2006**, *49*, 2969–2978.

(146) Hughes, J. D.; Blagg, J.; Price, D. A.; Bailey, S.; DeCrescenzo, G. A.; Ellsworth, R. V. D. E.; Fobian, Y. M.; Gibbs, M. E.; Gilles, R. W.; Greene, N.; Krieger-Burke, E. H. T.; Loesel, J.; Wager, T.; Whiteley, L.; Zhang, Y. Physicochemical drug properties associated with *in vivo* toxicological outcomes. *Bioorg. Med. Chem. Lett.* **2008**, *18*, 4872–4875.

(147) Lovering, F.; Bikker, J.; Humblet, C. Escape from flatland: increasing saturation as an approach to improving clinical success. *J. Med. Chem.* **2009**, *52*, 6752–6756.

(148) Ritchie, T. J.; Macdonald, S. J. F.; Young, R. J.; Pickett, S. D. The impact of aromatic ring count on compound developability: further insights by examining carbo- and hetero-aromatic and -aliphatic ring types. *Drug Discovery Today* **2011**, *16*, 164–171.

(149) Alelyunas, Y. W.; Empfield, J. R.; McCarthy, D.; Spreen, R. C.; Bui, K.; Pelosi-Kilby, L.; Shen, C. Experimental solubility profiling of marketed CNS drugs, exploring solubility limit of CNS discovery candidate. *Bioorg. Med. Chem. Lett.* **2010**, *20*, 7312–7316.

(150) Noe, M. C.; Gilbert, A. M. Targeted covalent enzyme inhibitors. *Annu. Rep. Med. Chem.* **2012**, *47*, 413–439.

(151) Dounay, A. B.; Anderson, M.; Bechle, B. M.; Campbell, B. M.; Claffey, M. M.; Evdokimov, A.; Evrard, E.; Fonseca, K. R.; Gan, X.; Ghosh, S.; Hayward, M. M.; Horner, W.; Kim, J.-Y.; McAllister, L. A.; Pandit, J.; Paradis, V.; Parikh, V. D.; Reese, M. R.; Rong, S.; Salafia, M. A.; Schuyten, K.; Strick, C. A.; Tuttle, J. B.; Valentine, J.; Wang, H.; Zawadzke, L. E.; Verhoest, P. R. Discovery of brain-penetrant, irreversible kynurenine aminotransferase II inhibitors for schizophrenia. *ACS Med. Chem. Lett.* **2012**, *3*, 187–192.

(152) Johnson, D. S.; Stiff, C.; Lazerwith, S. E.; Kesten, S. R.; Fay, L. K.; Morris, M.; Beidler, D.; Liimatta, M. B.; Smith, S. E.; Dudley, D. T.; Sadagopan, N.; Bhattachar, S. N.; Kesten, S. J.; Nomanbhoy, T. K.; Cravatt, B. F.; Ahn, K. Discovery of PF-04457845: a highly potent, orally bioavailable, and selective urea FAAH inhibitor. *ACS Med. Chem. Lett.* **2011**, *2*, 91–96.

(153) Potashman, M. H.; Duggan, M. E. Covalent modifiers: an orthogonal approach to drug design. *J. Med. Chem.* **2009**, *52*, 1231–1246.

(154) Moghaddam, M. F.; Tang, Y.; O'Brien, Z.; Richardson, S. J.; Bacold, M.; Chaturvedi, P.; Apuy, J.; Kulkarni, A. A proposed screening paradigm for discovery of covalent inhibitor drugs. *Drug Metab. Lett.* **2014**, *8*, 19–30.

(155) Johansson, M. H. Reversible michael additions: covalent inhibitors and prodrugs. *Mimi-Rev. Med. Chem.* **2012**, *12*, 1330–1344.

(156) Uetrecht, J. P. New concepts in immunology relevant to idiosyncratic drug reactions: the “danger hypothesis” and innate immune system. *Chem. Res. Toxicol.* **1999**, *12*, 387–395.

(157) Nakayama, S.; Atsumi, R.; Takakusa, H.; Kobayashi, Y.; Kurihara, A.; Nagai, Y.; Nakai, D.; Okazaki, O. A zone classification system for risk assessment of idiosyncratic drug toxicity using daily dose and covalent binding. *Drug Metab. Dispos.* **2009**, *37*, 1970–1977.

(158) Regina, A.; Demeule, M.; Che, C.; Lavalley, I.; Poirier, J.; Gabathuler, R.; Beliveau, R.; Castaigne, J. P. Antitumour activity of ANG1005, a conjugate between paclitaxel and the new brain delivery vector Angiopep-2. *Br. J. Pharmacol.* **2008**, *155*, 185–197.